AN EVALUATION OF QUANTITATIVE METHODS TO ESTIMATE ABUNDANCE OF NESTING CANADA GEESE IN THE HUDSON BAY LOWLANDS

A Thesis Submitted to the Committee on Graduate Studies

in Partial fulfillment of the Requirements for the Degree of Master of Science

in the Faculty of Arts and Science

TRENT UNIVERSITY

Peterborough, Ontario, Canada

Environmental & Life Sciences M.Sc. Graduate Program

September 2024

ABSTRACT

An evaluation of quantitative methods to estimate abundance of nesting Canada geese in the Hudson Bay Lowlands

Matthew Poppleton

Estimation of population abundance from samples has inherent practical challenges. Moreover, analytical methods to estimate abundance may vary in statistical assumptions and prediction uncertainties. I evaluated the performance of design-based and model-based methods to estimate Canada geese (*Branta canadensis*) abundance based on aerial fixed-width transect surveys in the Hudson Bay Lowlands, Canada. I evaluated Empirical Bayesian Kriging (EBK), areal interpolation and a ratio estimator on the basis of accuracy and precision using spatial point simulations. Untransformed EBK was the most accurate and precise, due in part, to its inherent handling of nonstationary distributions. The ratio estimator followed the same trends as EBK and, in some cases, had higher precision. Consideration of alternative analytical methods and their strengths and weaknesses is an important step in generating reliable information for population monitoring. Geostatistical approaches such as EBK have the benefit of providing spatially explicit mapping of abundance and reliable population estimates.

Keywords

Population ecology, spatial ecology, Canada goose, geostatistics, model-based inference, design-based inference, empirical Bayesian Kriging, areal interpolation, ratio estimator

Acknowledgments

I would like to begin by expressing my sincere gratitude to my supervisors, Dr. Glen Brown and Dr. Jim Schaefer, for their guidance and patience throughout my thesis. I appreciate the time you both allocated for our many update meetings. Thank you, Dr. Glen Brown for allowing me to pursue this project and for answering my countless questions about kriging and data analysis. Dr. Jim Schaefer, thank you for your expertise and valuable research suggestions. I would also like to thank my committee member Dr. Erin Koen for your valuable feedback.

Thank you, Kim Bennett and Rod Brook, for the opportunity to join you on the spring 2021 Canada goose aerial surveys and participate in the summer field work. To my lab mates: Gillian, Laura, Richard, Callie, Mihika, Dorothy, Chrystyn and Kapillesh, I am grateful for your feedback during our meetings. I would also like to extend my appreciation to the Trent Maps Data & Information Centre and the online ESRI community for their assistance whenever I was especially stumped from GIS and programming. I would also like to express gratitude to all my academic mentors, especially Dr. Jennifer Lund and Mr. Jeff Bradford for your advocacy during my educational journey.

A heartfelt thanks to my parents Patrice and David along with my brother, Adrian, for your unwavering support. Thank you to my partner Evangeline for all your support and working alongside me so many times. I cannot forget to thank my best friend Kirby, for always keeping in me good company with your calming presence and energetic activities.

Lastly, this research would not have been possible without the collaboration and support of the Mississippi Flyway Council, Ontario Ministry of Natural Resources and Forestry, Canadian Wildlife Service and the United States Fish and Wildlife Service.

Table of Contents

List of Figures

List of Tables

1.0 Introduction

Documenting changes in abundance of wildlife populations is essential for conservation and management. Counting all individuals in a population (e.g., Mech 1966; Peterson et al., 1998) may provide ideal data; however, complete counts are often too laborious and expensive to undertake at large spatial scales. In lieu of true censuses, population abundance can be estimated using wildlife surveys and a representative sample of the true population (Alisauskas et al., 2014; Lancia et al., 1994; McDonald 2004; Pearse et al., 2008). Estimates of population size can be sensitive to the choice of statistical model and how well the data fit underlying assumptions (Kéry 2002; Royle & Nichols, 2003; Peterson & Bayley, 2004; Dorazio 2007; McCallum 2008; Reed 2008; Tanadini & Schmidt, 2011). Selecting the ideal method to infer a parameter such as estimated population abundance is not always straightforward, as the analytical method depends largely on the survey design, parameters used, organisms studied and available resources (McCallum 2008).

Statistical inferences about population abundance often employ design-based or model-based methods (Dumelle et al., 2022). The design-based approach assumes that underlying population sizes are fixed and relies on random sampling; while the model-based approach uses spatial relationships and distributional assumptions to generate estimates and assumes that the underlying populations size are realizations of stochastic processes (Aubry & Francesiaz, 2022; Dumelle et al., 2022).

One class of model-based methods of particular interest is the use of geostatistical models that explicitly consider spatial relationships to estimate population size. Such geostatistical models assume spatial autocorrelation between sample units. One such geostatistical model,

simple Kriging models allow spatially explicit estimation of population characteristics and use a semivariogram to define how the similarity of a sampled parameter diminishes with distance. Simple kriging uses a single semivariogram to define the spatial covariance structure of sampled locations and to interpolate values in unsampled areas (Clark 1978). Empirical Bayesian kriging (EBK) extends this approach by accounting for the error in estimating the semivariogram model and simulating many semivariogram models rather than one semivariogram (Krivoruchko 2012; Krivoruchko & Gribov, 2019). These methods assume Gaussian distributed data; however, EBK offers flexible data transformations. If a transformation is applied with EBK, a simple kriging model is used instead of an intrinsic random function (Krivoruchko 2012).

Another common issue in population estimation pertains to the underlying distribution of the data. In particular, population surveys of animal counts will rarely have a Gaussian distribution. Areal interpolation is another geospatial interpolation method that interpolates data averaged over polygons, does not require a Gaussian data distribution, and can be used with discrete counts. The method can explicitly fit overdispersed Poisson data (Krivoruchko et al., 2011).

Nonstationarity of observations poses an additional challenge for accurate estimation of abundance, especially for mobile species. Nonstationarity is the assumption that data (e.g. the mean of an estimated parameter) change over time or space. An assumption common to many statistical estimation methods is that the true mean, and the semivariogram in the case of geostatistical methods, is the same at all locations in the data extent (in other words, stationarity or spatial homogeneity). However, natural populations may often exhibit complex spatial structure that violates such an assumption (Gribov & Krivoruchko 2020). For example, abrupt boundaries and gradual gradients in habitat quality may have different effects on animal

distribution and the spatial similarity of sampled observations. Of the methods considered here, EBK can account for moderately nonstationary data by using local models of subsets of the data and merging models, allowing for spatially varying parameterization of the spatial correlation structure (Krivoruchko 2012; Gribov & Krivoruchko, 2020). Failure to account for nonstationarity could bias population estimates; however, this aspect has not received much attention in wildlife survey design. Inaccurate estimates can be detrimental for conservation; population declines, or increases may go undetected. Design-based and geostatistical methods of abundance estimation differ in their ability to address these various assumptions; the consistency and bias among methods has not been fully investigated.

The population of Canada geese (*Branta canadensis*) in Southern Hudson Bay provides a useful case for assessing the methods of population estimation. Each spring, these birds migrate through the Mississippi Flyway and breed along the northern shores of Ontario and Manitoba of the Canadian subarctic (Luukkonen & Leafloor, 2017). Each spring, population surveys are conducted by recording the abundance of Canada geese from aircraft by adhering to line transects along the northern Ontario and Manitoba coastlines (Figure 1). These transects are generally 20 km long and roughly evenly spaced along the coastal survey area. All individual geese and breeding pairs are counted within 250 meters of each transect. Estimates of the breeding bird population from these surveys are used for for detecting trends in abundance and for setting harvest regulations (Luukkonen & Leafloor, 2017).

The Southern Hudson Bay breeding population of Canada geese are widely hunted across their full annual range, making population monitoring necessary to set sustainable harvest rates (U. S. Fish and Wildlife Service 2011). The population is managed cooperatively between the

U.S.A. and Canada (Luukkonen & Leafloor, 2017) and the effectiveness of harvest management depends on the accuracy of population estimates. Preliminary assessment of aerial survey count data indicated that the resulting population abundance estimates from these surveys were not consistent across modelling techniques. Specifically, differences in estimated abundance were evident among a design-based ratio estimator (Stehman & Salzer, 2000) and the model-based interpolation methods empirical Bayesian kriging (EBK; Krivoruchko & Gribov, 2019) and areal interpolation (Krivoruchko et al., 2011; Figure 2). A general correspondence in population trends among the methods was evident, but with upwards of a 20% discrepancy among estimates of population size. Without accurate population estimates, harvest management decisions could result in unexpected declines or overabundance of Canada goose populations. Overabundance can lead to ecological issues such as overgrazing, in which high density migratory goose colonies can limit productivity and foraging availability (Kuijper et al., 2009; Bazely & Jefferies 1986; Buij et al., 2017; Leafloor et al., 2000, Brook et al., 2015).

To compare these methods of goose population estimation, I examined the accuracy and precision of one design-based method and two geospatial methods. Design-based methods assume that abundance is a fixed number; uncertainty in the estimate is based on the selection probability of each sample rather than on spatial relationships (Aubry & Francesiaz, 2022). On the other hand, geospatial methods are model-based designs that use spatial relationships to predict abundance and that the population is assumed to come from a distribution (Aubry & Francesiaz, 2022).

In my thesis, as the design-based approach, I selected the ratio estimator (Stehman & Salzer, 2000). The ratio estimator uses computationally simple statistics to estimate population size,

where final estimates can be summarized as total counts per transect divided by the mean total area per transect (Stehman and Salzer 2000). Data based on quadrat sampling designs are typically collected under the assumption that sample areas are arranged across equal distances (Stehman & Salzer, 2000). For geese along Hudson Bay, the transects in this survey occur along unequal lengths within an irregular sample area; thus, traditional quadrat sampling may result in biased survey results. The transect density-based ratio estimator can also address this bias (Stehman & Salzer, 2000). The ratio estimator is computationally straightforward in comparison to EBK and Areal Interpolation, which employ geostatistical methods.

In my thesis, as the two geospatial methods, I selected empirical Bayesian kriging (EBK) and areal interpolation (Krivoruchko & Gribov, 2019; Krivoruchko et al., 2011). Kriging models allow spatially explicit estimation of population characteristics; these models use the spatial covariance structure of sampled locations to interpolate values in unsampled areas (Clark 1978). Empirical Bayesian kriging (EBK) is a specialized kriging population estimation model well suited for handling large-scale nonstationary spatial data such the Canada goose surveys (Krivoruchko 2012, Krivoruchko & Gribov, 2019). Out of the three models I selected, EBK is the only one capable of addressing spatial nonstationarity. Areal interpolation is another geospatial method that instead interpolates data averaged over polygons, does not require a Gaussian data distribution, can be used with discrete counts and is compatible with overdispersed Poisson data (Krivoruchko et al., 2011). Areal interpolation involves the reaggregation of data from a set of source polygons to a new set of target polygons. Areal interpolation can use discrete count overdispersed Poisson data (Krivoruchko et al., 2011), a circumstance that is common in surveys of animal abundance (Royle et al., 2005; Link & Sauer 1997; 2002; Caraco 1980).

The main objectives of my thesis are to evaluate the accuracy and precision of design-based and geospatial population estimators using simulated spatial points. I also applied these estimators to empirical Canada goose survey data collected from 2016 to 2021 (with the exception of 2020). I used the systematic fixed-width aerial transect survey of Canada goose breeding pairs to evaluate the performance of population estimators. Given that survey accuracy may depend on the distribution of animals (Green et al., 2022), I used simulated spatial points with 3 distributions to demonstrate the performance of the four abundance estimation models to predict population size, on the basis of accuracy and precision. These distribution types ranged from uniform to simulated realism: spatially balanced (uniformly distributed) to simple nonstationary (random clustering) and empirical nonstationary (clustering based on observed goose distributions and preferred habitat).

I anticipate that the accuracy of population estimates may vary among design-based and model-based methods in relation to their assumptions and to the sample design employed. EBK is well-suited for nonstationary data, and I predicted that it would be most accurate in the presence of strong nonstationarity. On the other hand, if the underlying Poisson data distribution is a strong influencing factor for accurate population estimates, areal interpolation may be the most accurate. In contrast, if improved Gaussian data transformation and nonstationarity are strong factors, a transformed EBK model (EBKT) may be most accurate. Finally, if geospatial relationships at this scale are not important, I anticipate that the ratio estimator will be the most accurate. Clarifying uncertainties in the accuracy and strengths or limitations of these methods should help ensure effective use of survey effort to improve detection of population changes and distribution and allow for improved predictions and timely responses to future population fluctuations.

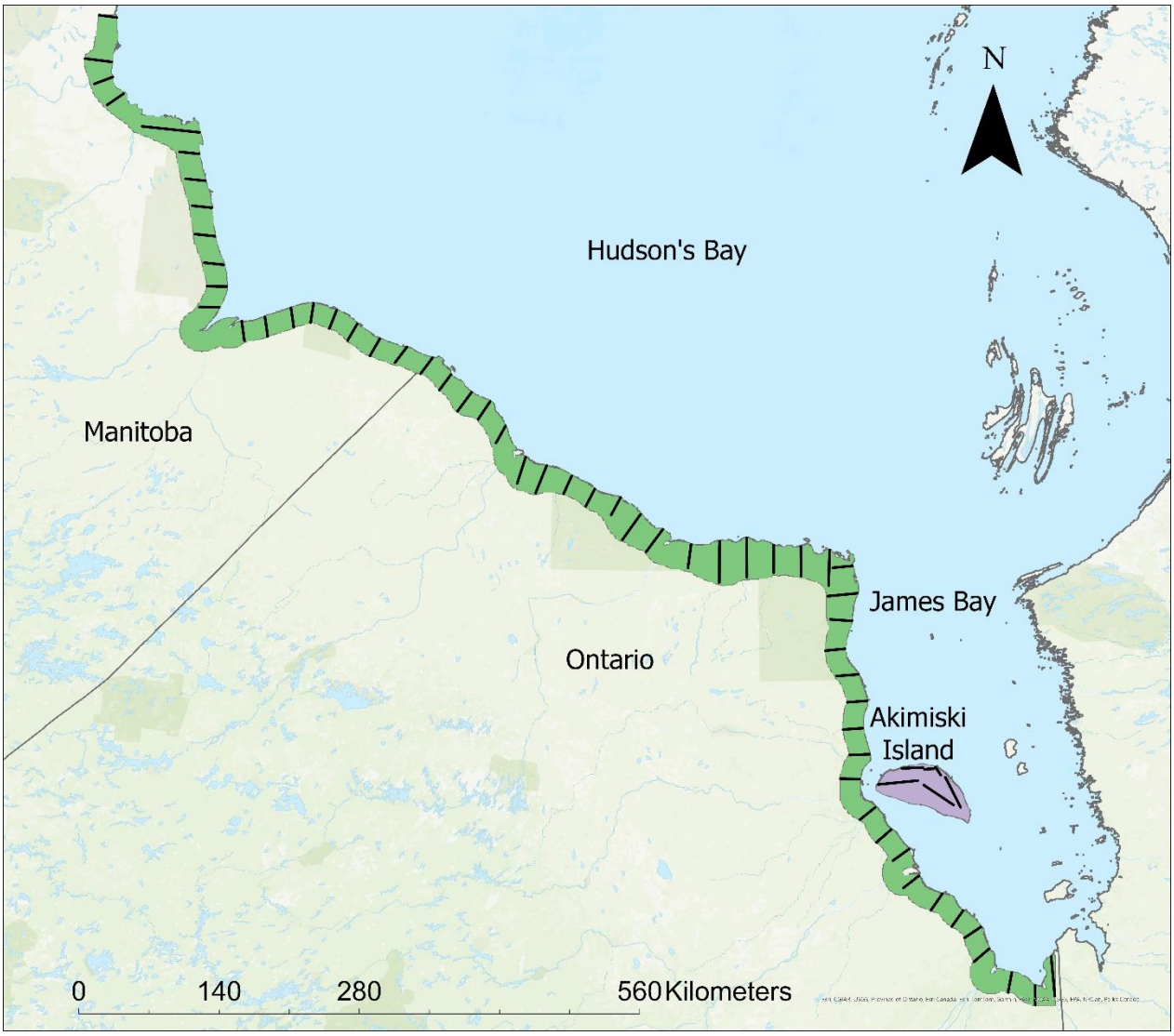

Figure 1. The study area for the Mississippi Flyway Canada Goose (*Branta canadensis*) surveys, northern Ontario, Nunavut and Manitoba, Canada. Green represents the mainland study area boundary, purple represents the Akimiski Island study area boundary. Lines represent transects for aerial surveys.

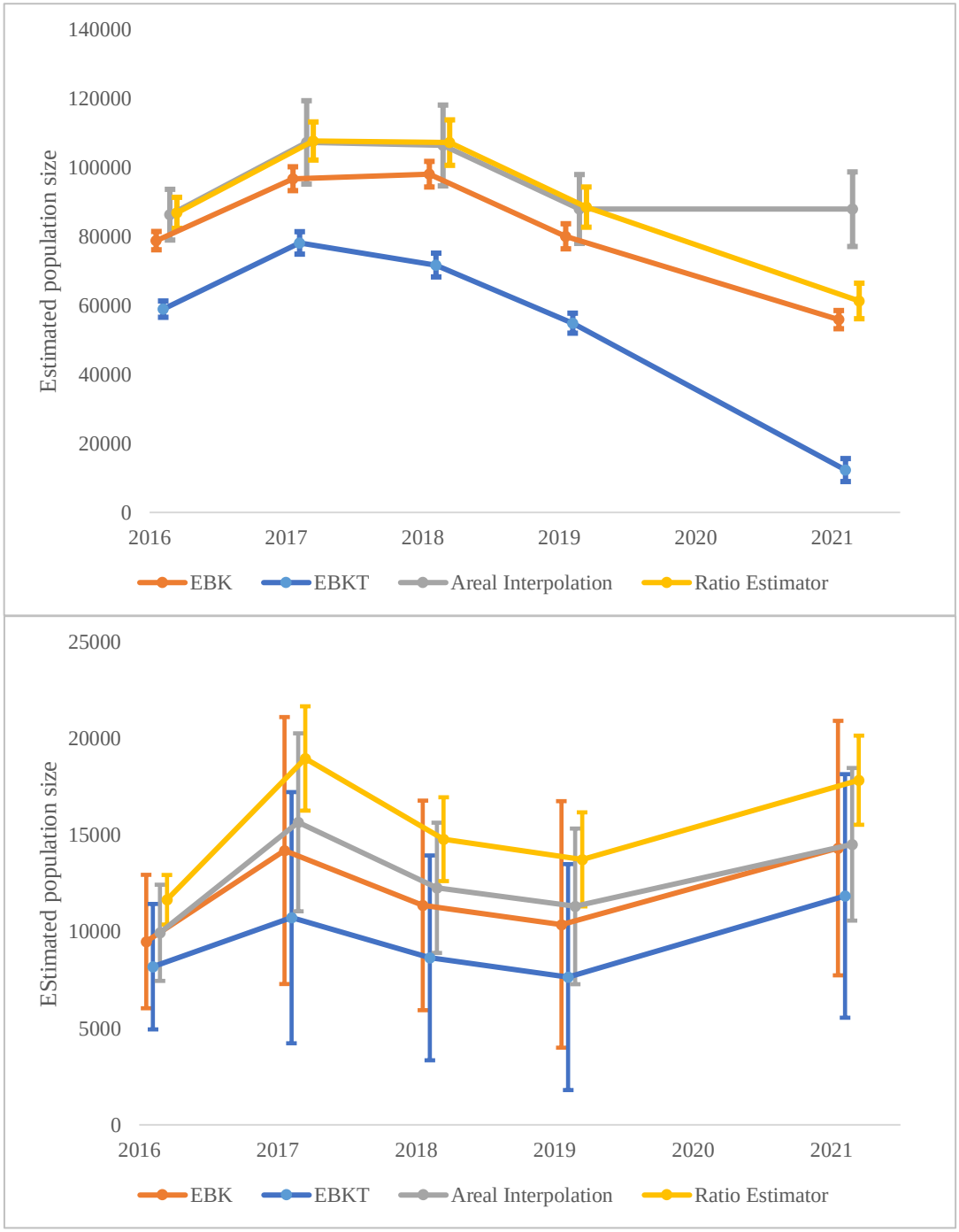

Figure 2. Population estimates for Canada geese (*Branta canadensis*) in the Mississippi Flyway, 2016-2019 and 2021, based on design-based and geospatial methods. The design-based method is the ratio estimator (Stehman & Salzer, 2000), and the geospatial methods are untransformed and transformed empirical Bayesian kriging (transformed and EBK and EBKT respectively; Krivoruchko & Gribov, 2019), and areal interpolation (Krivoruchko et al., 2011). The top panel depicts population estimates for the mainland, while the bottom panel depicts population estimates for Akimiski Island. Bars represent standard error.

2.0 Methods

2.1 Data collection

My evaluation of methods focused on aerial breeding pair population surveys for Canada geese in the subarctic region of the Mississippi Flyway. Canada geese in this region have been surveyed each spring by the Ontario Ministry of Natural Resources and Forestry (MNRF) on behalf of the Mississippi Flyway Council, a joint group formed in 1952 to monitor game bird populations along this migration route (Luukkonen & Leafloor, 2017). The group encompasses federal, state, and provincial governments, including the Canadian Wildlife Service and the United States Fish and Wildlife Service (Brook et al., 2018). In the spring of 2021, I joined the field staff that take part in these surveys to study the methodology in person.

The field methods are generally consistent year to year. Surveys are conducted in late May to early June, during the breeding to nesting period. The surveys follow fixed-width line transects that are roughly evenly spaced and perpendicular to the coast (Figure 1). The transects are flown with a Twin Otter fixed-wing aircraft. As the aircraft flies over each geolocated transect, one observer on the left and one observer on the right record sightings of Canada geese within a 250-m of the flight line. Before the observations begin, a test transect is flown for each observer to calibrate this transect width. Sightings are recorded for all individual geese, breeding pairs and groups; indicated breeding pairs are represented by non-paired geese and individuals in odd numbered groups; sightings are timestamped and later geolocated after the survey is complete. The information recorded includes time, date, species, grouping, sex (a pair indicates 1 male and 1 female [otherwise unknown]), behaviour (e.g. flying, on nest, in water, on ground), observer and transect information, and coordinates. Surveys are typically done two weeks into the Canada

geese incubation period, but timing can vary depending on phenology and snowmelt. The most southern transects, along the coast of James Bay, are sampled one week before the more northerly transects (Figure 1; Brook, R. personal communication). This chronology of sampling is done to adjust for snowmelt and subsequent variations in geese nesting periods. During any one year, the observers are often the same individuals, to reduce observation bias.

The sample area includes the James Bay and Hudson Bay coastline, from the Quebec-Ontario border across Ontario into northern Manitoba, and Akimiski Island, Nunavut (Figure 1). During 1989-2016, the aerial transects were distributed further inland from the coast, using systematically scattered line transects. This was done to collect abundance information on the interior breeding and nesting grounds. In 2016, the study area was redesigned to use systematic, parallel line transects perpendicular to the coastline, limited to areas with highest goose density. The transects for Akimiski Island, however, were not relocated to use the same systematic approach. Instead, random transects were removed from the interior of the island; five transects were kept in the northern high-density area and three transects were introduced to the southern low-density area. The island transects are parallel to the coastline and are positioned from judgmental sampling (Figure 1).

2.2 Methods used to estimate population abundance

To analyze these population data, I selected three abundance-estimation models: empirical Bayesian kriging, areal interpolation, and the ratio estimator (Krivoruchko & Gribov, 2019; Krivoruchko et al., 2012; Krivoruchko et al., 2011; Stehman & Salzer, 2000). Furthermore, I evaluated empirical Bayesian kriging models with and without transformation (EBKT and EBK, respectively).

The design-based approach that I selected was the ratio estimator (Stehman & Salzer, 2000). Data based on quadrat sampling design are typically collected with the assumption that sample areas are arranged across equal distances (Stehman & Salzer, 2000). For geese along Hudson Bay, the transects in this survey occur along unequal lengths within an irregular sample area (Figure 1) and thus traditional quadrat sampling may result in biased results. The transect density-based ratio estimator can address this bias (Stehman & Salzer, 2000; Brook et al., 2018). The ratio estimator population estimates were calculated as:

$$Estimated\ population = Study\ area\ size\ \times \frac{Mean\ goose\ pair\ count}{Mean\ transect\ \ area}$$

The two geospatial methods that I selected were empirical Bayesian kriging (EBK) and areal interpolation (Krivoruchko & Gribov, 2019; Krivoruchko et al., 2011). Kriging represents a class of geostatistical models to interpolate spatial data from areas that have not been directly sampled, using data from sampled locations (Cressie 1993; Krivoruchko 2012). Kriging measures the similarity between points between increasing distances and is derived from a semivariogram, which determines data spatial dependency over these increased distances (Clark 1978). However, classical kriging models typically use one semivariogram, which may not be representative of large-scale ecological data (Krivoruchko 2012). To account for such circumstances, empirical Bayesian kriging (EBK) generates multiple semivariograms to address the uncertainties in these classical kriging models (Krivoruchko 2012). EBK can automatically transform input data to a Gaussian distribution EBK which is robust to nonstationary data (Gribov & Krivoruchko, 2020). This was the basis of my EBKT simulation. Notably, the transformation and semivariogram types can be set to different parameters.

EBK and EBKT were calculated using ArcGIS Pro's Geostatistical Analyst, via the ArcPy library, using the EmpiricalBayesianKriging_ga function (ESRI 2024a; 2024b). I ran each simulation with consistent parameters (Appendix 8; 9). This process produced prediction density surfaces which were then converted to rasters. To get the population predictions, I multiplied the raster mean by the total area (km^2) of the respective study area.

In my assessment of the untransformed EBK method, I used a transformation of "None", and a semivariogram model of "Power". In this case, the parameters of the semivariogram were estimated using a Power function and restricted maximum likelihood (REML; ESRI 2024c). The power semivariogram model (ESRI 2024c; Krivoruchko 2012) is calculated using the parameters nugget (y-intercept), b (slope) and α (power):

$$\gamma(h) = Nugget + b|h|^{a}$$

In my assessment of the Empirical Bayesian kriging transformed (EBKT) estimator, I used an "Empirical" transformation and a "K-Bessel Detrended" semivariogram model. The empirical transformation setting applies a normal score transformation, converting the data to a Gaussian process (Krivoruchko 2012). The Detrended K-Bessel semivariogram model detrends values by applying a first-order trend removal before computing the semivariogram (ESRI 2024c). The K-Bessel semivariogram model (Johnston et al., 2003) is calculated as:

$$\gamma(\mathrm{h};\theta) = \theta_s \left[1 - \frac{\left(\Omega_{\theta_k}\|\mathrm{h}\|/\theta_r\right)^{\theta_k}}{2^{\theta_k-1}\Gamma(\theta_k)} k_{\theta_k}\left(\Omega_{\theta_k}\|\mathrm{h}\|/\theta_r\right)\right] \text{ for all h,}$$

where θ, θ_r and θ_k are non-negative values. The parameter Ω_{θ_k} is computed numerically such that $\gamma(\theta_r)$=0.95 for any given θ_k. The parameter $\Gamma_{(\theta_k)}$ represents the gamma function:

$$\Gamma(\gamma) = \int_0^\infty x^{y-1} \exp(-x)\, dx$$

The parameter k_{θ_k} represents the modified Bessel function (Abramowitz & Stegun, 1965) of the second kind of order θ_k (ESRI 2024c; Johnston et al., 2003).

The other model-based geostatistical method I used for my analysis was areal interpolation (Krivoruchko et al., 2011). Areal interpolation is a kriging interpolation method that reaggregates spatial data from polygons features to a prediction surface with the option of reaggregating these data to a new set of polygon features (Krivoruchko et al., 2011; ESRI 2024d). Since areal interpolation uses polygon input features, the method can handle input polygon size irregularities. Depending on the model selected, Areal interpolation can also handle different types of input data including overdispersed Poisson data (Krivoruchko et al., 2011)

For my areal interpolation workflow, I used the overdispersed Poisson areal kriging model (Krivoruchko et al., 2011). This model was computed using the ArcGIS Pro Geostatistical Analyst areal interpolation dataset type "event count" (overdispersed Poisson counts; ESRI 2024d). This dataset type best fits count data within defined areas and units of time, whereas a goose sighting would an event. The resulting prediction surface depicts a the of the likelihood of locating individuals across space (ESRI 2024d). The Canada goose survey transect samples were used as the polygon input to generate prediction surfaces that were then reaggregated to a new polygon of the total study area. Final abundance estimates were gathered from each final polygon prediction value.

To generate prediction surfaces, interpolation covariance models were manually adjusted for each model run using ArcGIS Pro's Geostatistical Analyst Wizard. This was done by adjusting

the “Lag Size” and “Lattice Spacing” parameters until as many empirical covariance averages were within the confidence intervals as possible (ESRI 2024d). These parameters varied among simulations; nonetheless “Lag Size” was typically 500-2000 and “Number of Lags” was typically 10-15. This manual modelling was somewhat laborious and thus was a constraint on the number of repeated simulations I could generate.

To apply these geostatistical methods (EBK, EBKT, areal interpolation), I partitioned the transects into equal-sized quadrats as a means to take advantage of the spatially explicit location information for counts. This information is not inherently available under the design-based probability sampling analysis paradigm for the transects.

I calculated the ratio estimator via Microsoft Excel and Python scripts. This design-based method uses each transect as a sample unit; each transect is about 20 km in length. In the case of the geospatial estimators, the partitioned quadrats were set to the size of 2000 m by 500 m. This partitioning created sample blocks of 1 km^2 that captured spatial variation in goose abundance. I inspected the distribution of these data using relative frequency histograms.

I divided my assessment into two regions for analysis due to differences in sample design and observation density. The mainland study area extended along the coastline of Hudson Bay and James Bay, in northern Ontario and Manitoba. The second, much smaller study area was Akimiski Island, Nunavut (Figure 1). The the mainland study area had a total area of 40269 km^2 and Akimiski Island had a total area of 3015 km^2.

2.3 Spatial point simulations

In my simulations of goose distribution, I applied three forms of distribution with increasing degrees of nonstationarity: spatially balanced, simple nonstationary, and empirical nonstationary, (Figure 3). For each scenario, I generated points (each representing one animal) within both the Mainland and Akimiski Island study areas boundaries.

The spatially balanced simulations were based on animals distributed semi-uniformly across each study area and are based on spatially balanced sampling theory (Theobald et al., 2007; Stevens & Olsen 2004). Spatially balanced survey designs compute probability-based, evenly distributed sample locations and uses an algorithm called the Reverse Randomized Quadrant-Recursive Raster to map 2D space to 1D space. This algorithm results in sample designs with a low variance of polygon area surrounding each sample location (Theobald et al., 2007). Inclusion probability values are also set to specify the probability selecting each sample location (Theobald et al., 2007; ESRI 2024d). The resulting spatially balanced distribution distributes a preset amount of sample point locations proportionally across the study area while allowing for randomization (Theobald et al., 2007; ESRI 2024d;).

The spatially balanced simulations were computed using the "Create Spatially Balanced Points" geoprocessing tool in ArcGIS Pro, where each spatially balanced randomly positioned point represented a simulated bird. I used a randomization seed of 0 for each run to generate random point locations. The distances between points were not equal at all locations due to randomization and the irregular study boundaries, though these points exhibit a relatively uniform distribution across the large-scale study area (Figure 3; Appendix 1; Appendix 2).

The simple nonstationary simulation added a degree of nonstationarity, by grouping points into randomly distributed clusters across the simulation area. This was used to create a randomly clustered dataset that was independent of land features (Figure 3; Appendix 1; Appendix 2). While the location of each cluster was random, parameters were set for the minimum and maximum points per cluster, cluster radius, and minimum distance between each point. Minimum and maximum points per cluster were set to 20 and 50 points respectively; minimum, and maximum cluster radius were set to 1000 m and 5000 m respectively; a minimum point distance was set to 1 m. The simple nonstationary simulation was generated using Python and ArcPy.

Canada geese exhibit higher clustering and density in areas of high habitat quality along the coast, with decreased density moving inland in relation to habitat (Reiter et al., 2013). For the empirical nonstationary simulation, I generated and distributed points using weighting factors based on proximity to water bodies and real goose survey data (Figure 3; Appendix 1; Appendix 2). This was accomplished by using a weighting layer generated by multiplying raster distance to lakes and Canada goose density, using R (R Core Team 2023) and the raster function from the Raster package (Hijmans 2023), before importing the points to ArcGIS for geoprocessing. Distance to water was used as a habitat variable as geese tend to be more abundant in the proximity of water bodies (McAlister et al., 2017). This weighting resulted in a more realistic distribution of points with less of a smooth gradient from high to low-density areas than the simple nonstationary simulation (Figure 3).

To assess how the accuracy of each population estimator and simulation set might change in relation to animal abundance, I generated one high and one low-count population for each study area and simulation run. For the mainland, the high and low counts were 100,000 and 50,000

geese. These numbers reflect realistic ranges in abundance based on expert opinion and recent population estimates (Figure 2; Brook et al., 2018). For Akimiski Island, I chose scaled-down counts relative to the mainland, reflecting the difference in study area size. For my analysis, I set the Akimiski high and low counts to 7,500 and 3,750 geese (Figure 2). The total number of generated points represented the 'true' population size, to which I compared estimates of abundance generated from the three estimation methods.

I determined counts for each simulation by totalling points within 250 m of each transect for the ratio estimator and inside each quadrat for the geospatial models. I generated points from each of the three distributions 10 times for each population estimation model and population size. To evaluate precision, I computed the standard errors for areal interpolation and the ratio estimator, and an approximate standard error for EBK and EBKT. Each method generates this standard error via a different process. The design-based ratio estimator uses a standard statistical approach to generate standard error while the geospatial methods calculated standard error using ArcGIS features. The ratio estimator calculates standard error as the square root of the estimated variance, where estimated variance is calculated as:

$$\left(\frac{1}{mean\ sample\ area^2} * \left(\frac{\left(\frac{study\ area\ width}{0.5} \right) - n}{\frac{study\ area\ width}{0.5}} \right) * \left(\frac{(\sum total\ count^2)^2}{n} \right) \right)$$

For the geospatial methods, areal interpolation in ArcGIS Pro provides a standard error for the predicted abundance within and between each input polygon feature, generates a prediction surface, and then reaggregates this error back to quadrat polygon features (ESRI 2024d). Unlike

areal interpolation, the ArcGIS Pro raster output for an EBK prediction surface includes standard deviation of the total population of raster cell predicted values. To adjust for the differences among methods in sample error estimation, I calculated an approximation of standard error by dividing the standard deviation by the square root of the number of sample units in the study area, multiplied by the study area size in square kilometers – i.e., area X $\left(\frac{SD}{\sqrt{n}}\right)$. I then calculated the standard error from each of these methods was then multiplied by the total study area size (40269 km^2 for the mainland; 3015 km^2 for Akimiski Island).

To access accuracy, the simulated populations were tested for significant differences using the Python libraries Pandas data frames and Numpy statistical functions (McKinney 2010; Harris et al., 2020). Three significance tests were computed using different functions from the SciPy library. First, to test for significant differences for the simulation mean population estimates I computed 1-sample t-tests using the SciPy function ttest_1samp (Virtanen et al., 2020). Second, to test for significant differences between the high and low simulated population sizes, independent 2-sample t-tests were computed using the SciPy function ttest_ind (Virtanen et al., 2020). lastly, test for significant differences across survey data estimates z-score tests were computed using the; 2-tailed values p-were then generated using the SciPy scipy.stats.norm survival function (Virtanen et al., 2020).

2.4 Spatial point simulation analysis

To assess the degree of clustering of each simulation scenario, I applied the Morisita index (I_d) on the 10-run average for each method (Figure 5). The Canada goose survey data was computed using counts per quadrat for the years 2016-2021. I applied the unstandardized Morisita's index; where I_d from 0-1 represents a uniform distribution, and $I_d > 1$ indicates

clumped patterns – the likelihood of two randomly selected individuals appearing in the same sampling unit (Sólymos 2022). I calculated the Morisita index using the dispindmorisita function from the vegan: Community Ecology R package (Sólymos 2022). Additionally, to measure the spatial autocorrelation of counts per quadrat for each simulation I plotted the Moran's I index as a correlogram. The correlograms were generated using the spdep package in R, via the sp.correlogram function (Pebesma & Bivand, 2023). Shapefiles consisting of the 10-run average counts per quadrat were used as input to generate neighbours with the poly2nb function using default settings; the average counts per quadrat were used as the variable of interest for the correlograms (Pebesma & Bivand, 2023; Figure 6). Lastly, to assess the realism of simulation data distributions compared to the real goose observation dataset, I created frequency distribution analysis was performed on the number of geese per quadrat, using R libraries tidyverse and xlsx (Wickham et al., 2019; Dragulescu & Arendt, 2020; Figure 7).

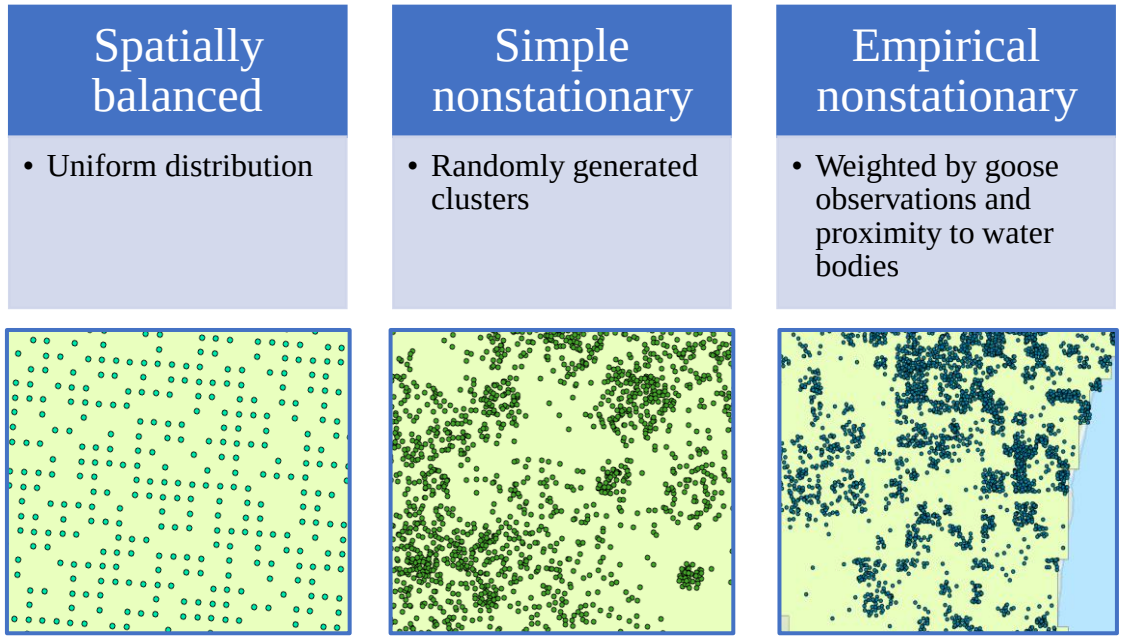

Figure 3. Spatial point examples of the three simulated distributions of animals, with increasing degrees of realism, based on increasing clustering and nonstationarity.

3.0 Results

3.1 Accuracy and precision of the population estimators

Regardless of the simulated animal distribution, the population sizes from the four estimators were similar, for both the mainland and Akimiski Island (Figure 4; Appendix 6). A two-sample t-test indicated no significant differences when comparing the high (mainland 100,000; Akimiski Island 7,500) and low (mainland 50,000; Akimiski Island 3,750) population sizes for each simulation type ($t > 76.65$, $df = 9$, $p > 0.05$). The mainland simulations had similar accuracy regardless of population size, with the exception of the simple nonstationary simulation where differences were present among all population estimators except EBKT. The mainland simple nonstationary 100,000-population simulation underestimated by an average of -2.84% across EBK, areal interpolation and the ratio estimator, while the 50,000-population simulation underestimated abundance by an average of -2.56% for these estimators. The EBKT estimate was closer to the true population (-21%) in the 100,000 simple nonstationary simulation than the 50,000 estimate (-36%).

On Akimiski Island, the results were comparable between simulation population sizes. The 3,750 and 7,500 population sizes had similar accuracy to the mainland's population sizes. Similar to the mainland, Akimiski Island's EBKT estimator using the simple nonstationary simulation was also more accurate at the large population size (-12.9%), than at the low population size (-43.3%). On Akimiski Island, the EBK was the most accurate at estimating population size for the simple nonstationary simulation, whereas in the areal interpolation had higher accuracy using the spatially balanced and empirical nonstationary simulations. However, these differences were marginal: the areal interpolation estimator for the empirical nonstationary simulation was more

accurate than EBK by just 0.2%; areal interpolation using the spatially balanced averages was more accurate than EBK by only 2.7%. On Akimiski Island, as on the mainland, the transformed empirical Bayesian kriging (EBKT) had the lowest accuracy of the methods employed (Figure 4).

In the mainland spatially balanced simulation, all the population estimates were reasonably accurate, with differences of <1%; this was not unexpected due to the uniformly distributed points. Similarly, all the estimators using the spatially balanced simulation were not significantly different from the true population size ($t < 2.07$, $df = 9$, $p > 0.05$). For the mainland simple nonstationary simulation, the EBK estimator was slightly more accurate than the ratio estimator and the areal interpolation simulations (-2.3%; -3%; -3.2% respectively). The EBK estimator was also not significantly different from the simulated population abundance ($t = -1.86$, $df = 9$, $p = 0.1$) for the simple nonstationary simulation; the EBKT estimator ($t = -22.56$, $\underline{df} = 9$, $p < 0.001$), ratio estimator ($t = -2.54$, $df = 9$, $p < 0.001$) and areal interpolation estimators ($t = -2.79$, $df = 9$, $p = 0.02$) were significant. Lastly, for the mainland empirical nonstationary simulation, the EBK estimator was the most accurate albeit with a slight overestimation (0.7%). For the empirical nonstationary simulation, EBK was the only estimator whose average was not significantly different than the true population size ($t = 1$, $df = 9$, $p = 0.34$). In contrast, the empirical nonstationary areal interpolation and ratio estimators both overestimated abundance by close to 10,000 individuals (or about 10% of the population).

Some simulation outcomes differed on Akimiski Island (Figure 4). The spatially balanced simulations all had similar accuracy across methods but slightly underestimated the true abundance. For the Akimiski Island spatially balanced and simple nonstationary simulations, the majority of the estimators were significantly different from the true population size ($t < 4.52$, $df =$

9, $p < 0.05$); with the exception of the simple nonstationary simulation estimates ($t < 1.13$, $df = 9$, $p > 0.05$) and the spatially balanced simulation areal interpolation estimate ($t = -1.86$, $df = 9$, $p = 1$).

For the simple nonstationary simulation on Akimiski Island, the EBK estimator was the most accurate although it marginally overestimated abundance by 0.8%. Areal interpolation and the ratio estimator overestimated abundance with increasing bias, respectively (2.4%; 4.8%). As for the empirical nonstationary simulation, EBK and areal interpolation underestimated the true population size by nearly 850 individuals (-11.9% and -11.8% respectively), while areal interpolation overestimated to a similar degree (10.8%). The EBKT estimator underestimated the population size for both simple and empirical nonstationary simulations across the mainland and Akimiski Island simulations. This was shown to the greatest degree with the empirical nonstationary simulation, underestimating abundance by -26.2% on the mainland and -29.8% for Akimiski Island.

Regarding the precision of these methods, EBK demonstrated the lowest standard error and thus highest precision, followed by the ratio estimator and lastly areal interpolation (Figure 4). Indeed, in the case of the uniform distribution, areal interpolation was appreciably less precise than the other methods. Across the 3 simulations, precision generally decreased with increased stationarity. Not unexpectedly, the spatially balanced simulation tended to have the lowest standard error, followed by the simple nonstationary simulation and the empirical nonstationary simulation for both the mainland and Akimiski Island.

3.2 Clustering & spatial autocorrelation

As expected, among the three artificial population distributions, the empirical nonstationary simulation had the highest degree of clustering, followed by simple nonstationary and spatially balanced with the lowest degree of clustering (Figure 5). Based on Morisita's Index, the empirical nonstationary point distributions most closely resembled the real data with respect to the degree of clustering ($2 < Id < 3.5$; Figure 5). The empirical nonstationary simulation exhibited higher clustering on the mainland than on Akimiski Island. The empirical nonstationary simulation exhibited the highest degree of spatial autocorrelation, followed in the same order by the simple nonstationary simulation then the spatially balanced simulation (Figure 6). From the Moran's I correlogram, the empirical nonstationary simulation displayed significant spatial autocorrelation for the first 8 lags for the mainland and for the first 4 lags for Akimiski Island. The mainland simple nonstationary simulation displayed significance for only the first 2 lags and the Akimiski Island simple nonstationary simulation displayed significance for only the first lag. As expected, the spatially balanced simulation did not exhibit significant autocorrelation across all 10 lags (Figure 6).

3.3 Frequency distributions

The frequency distribution of the real data demonstrated a high degree of skew towards counts of zero and one (Figure 7). As expected, of a near uniform distribution, the spatially balanced simulation had the distribution that most closely resembled normality. The frequency distributions of the simple and empirical nonstationary situations were more similar to the real data distribution, showing a positive skew, but with slight differences. The empirical nonstationary simulation better resembled the frequency of low counts per quadrat for the real

mainland data, whereas the mainland high counts per quadrat of the real data (the tails of the distribution; Figure 7) were more similar to the distribution for the simple nonstationary simulation. In other words, while the empirical nonstationary simulation better resembled the zero-inflation of the real data, this simulation also had more transects with higher counts than the real data. This pattern was not evident on Akimiski Island, as both simple and empirical distributions closely matched the frequency distributions of the real data.

3.4 Mississippi Flyway Canada goose population trends 2016-2021

During 2016-2021, average population estimates generally followed the same trends on both mainland and Akimiski Island (Figure 2). For the mainland and Akimiski Island, the ratio estimator generally produced the highest estimates, followed by areal interpolation, EBK and EBKT. Moreover, among the four methods, the rank order of the population estimates were similar to the results from the simulations, particularly for the mainland empirical nonstationary scenario.

Some year-to-year changes were evident on the mainland. From 2016-2021, the areal interpolation estimator did not reveal any significant annual changes in abundance ($z < 1.48$, $p > 0.05$). Compared to 2016, EBK, EBKT and the ratio estimator indicated significant population growth by 2017, with an average increase of +26% ($z < 4.78$, $p < 0.001$), but with no significant change in numbers the following year. However, by 2019 all survey estimates (except areal interpolation) indicated the converse, with an average decrease of -20% ($z < -2.13$, $p < 0.05$), which appeared to continue to 2021, with a further decrease of 35%. Lastly between 2019 and 2021, all mainland survey estimates were significant ($z < -3.50$, $p < 0.001$) except areal interpolation and on average they decreased by -46%. In contrast, the Akimiski Island ratio

estimator in 2017 was the only population estimator to exhibit a significant change in population size during 2016-2021 with an increase of 63% ($z = 2.45$, $p = 0.01$).

The rank order of the results among the estimators was generally unvarying. EBK produced estimates significantly different from all EBKT estimates, the 2016-2017 ratio estimator and the 2021 areal interpolation estimates. Among these estimators, for all survey years and for both the mainland and Akimiski Island, EBKT consistently produced the lowest estimates. On the mainland, EBKT estimates had the highest precision and were significantly different from the other estimators, but these patterns were not present for Akimiski Island. The EBK estimator and the ratio estimator followed each other closely; both methods revealed significant ($p < 0.001$) increases from 2016-2017 (+23%, $z = 4.12$; +24%, $z = 2.92$) and declines from 2018-2019 (18%, $z = -3.46$; 17%, $z = -2.13$) and 2019-2021 (-30%, $z = -5.37$; -31%, $z = -3.50$).

On the mainland with the exception of 2021, the areal interpolation estimator and the ratio estimator had very similar estimates and no significant differences. Areal interpolation was only significantly different from 2021 the EBKT estimate and the 2021 ratio estimator. The areal interpolation estimator exhibited a relatively high average standard error (10394) in comparison to the other estimators (5522 ratio estimator; 3225 EBK; 3059 EBKT). The ratio estimator was significantly different from the 2016-2017 EBK estimates, the 2021 areal interpolation estimate and all EBKT estimates.

For Akimiski Island, all estimators had overlapping standard errors and consequently none of the population estimates on were significantly different from each other. On the island EBKT estimator produced the highest standard error (5754) followed closely by EBKT (5444) then areal interpolation (3691) and lastly the ratio with the lowest average standard error (2180).

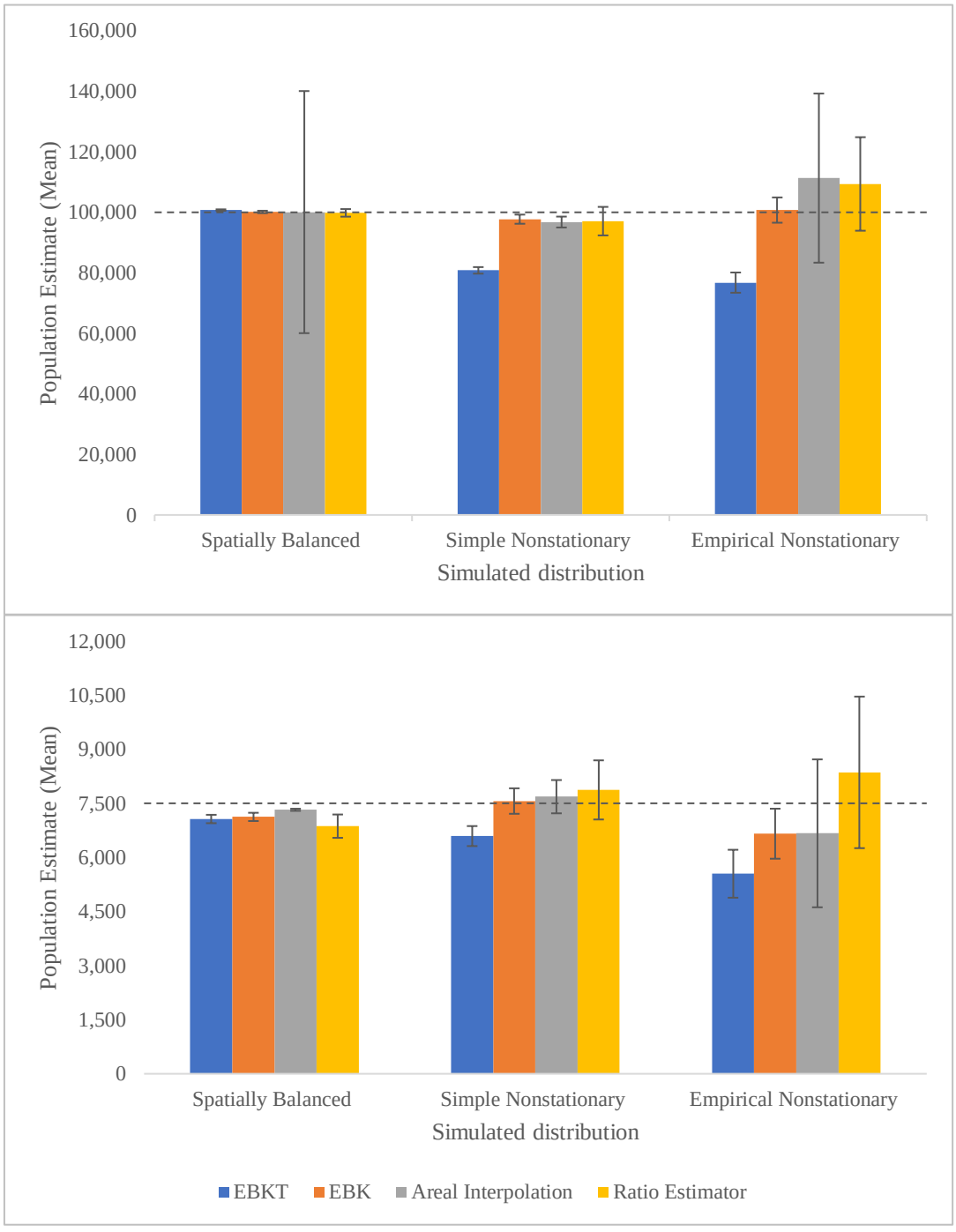

Figure 4. Mean population estimates averaged from 10 simulations for each of four population estimators and three simulated animal distributions. The error bars represent the standard error. The top panel depicts the mainland estimated population sizes using a simulated population of 100,000 points (dashed line), while the bottom panel depicts the Akimiski Island estimated population size using a simulated population of 7,500 points (dashed line).

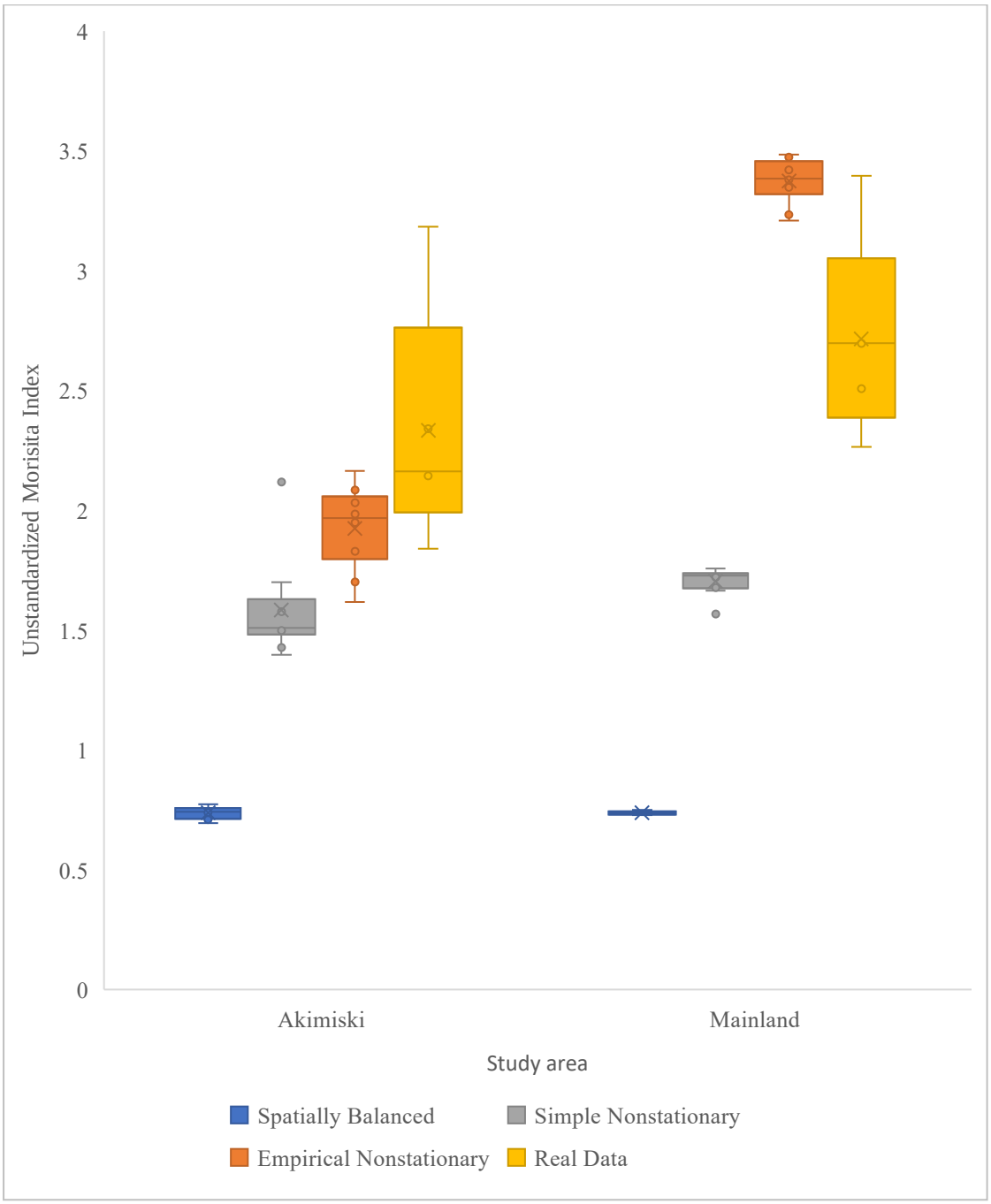

Figure 5. The unstandardized Morisita index of dispersion for each point simulated distribution on the mainland and Akimiski Island, indicating the degree of clustering for each simulation as well as the real observations of geese, 2016-2021. An I_d between 0-1 indicates uniform distributions while higher values of 0 to *n* indicate clumped distributions (Sólymos 2022).

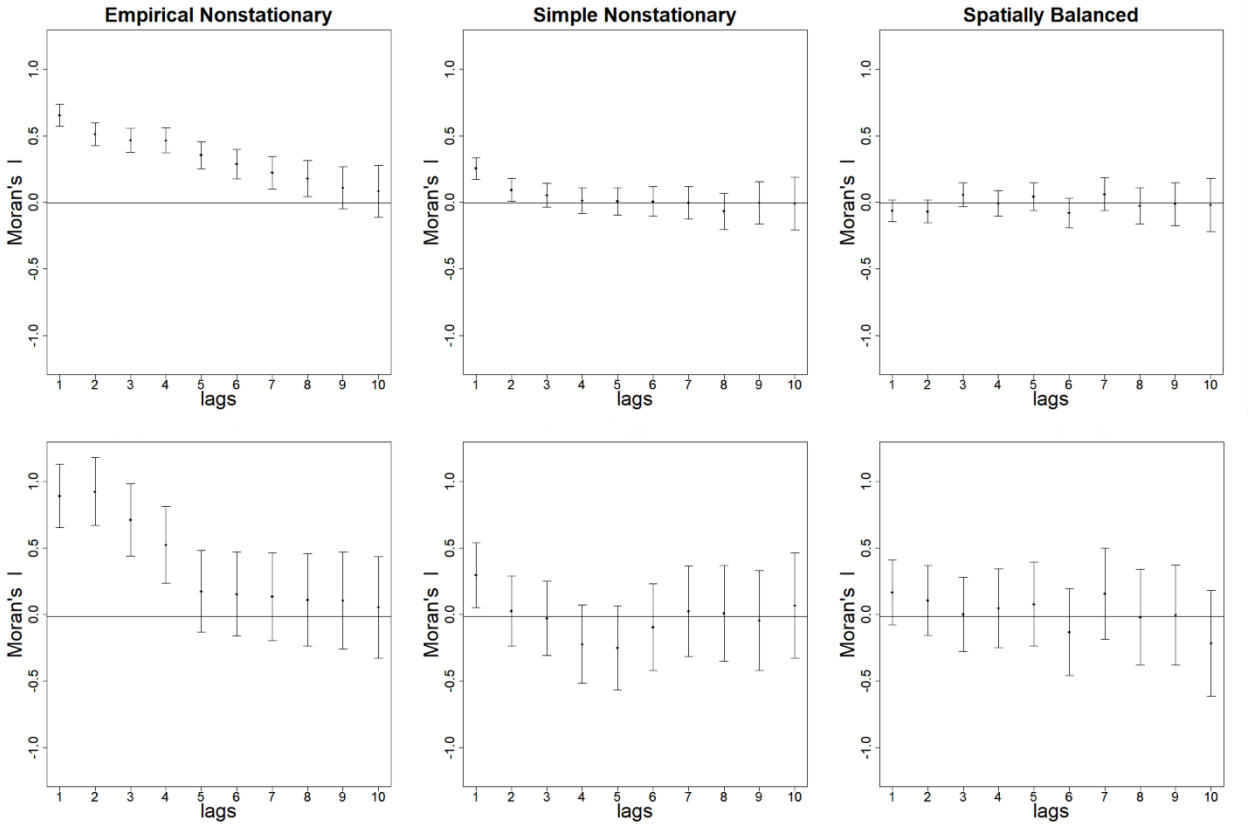

Figure 6. Moran's I index for each simulated distribution on the mainland and Akimiski Island, indicating the degree of spatial autocorrelation, for the average observation count per sample units for each simulation (Pebesma & Bivand, 2023). The top panels depict the mainland simulation of 100,000 birds; the bottom panels depict the Akimiski Island simulation of 7,500 birds. Error bars represent the standard deviates of Moran's I.

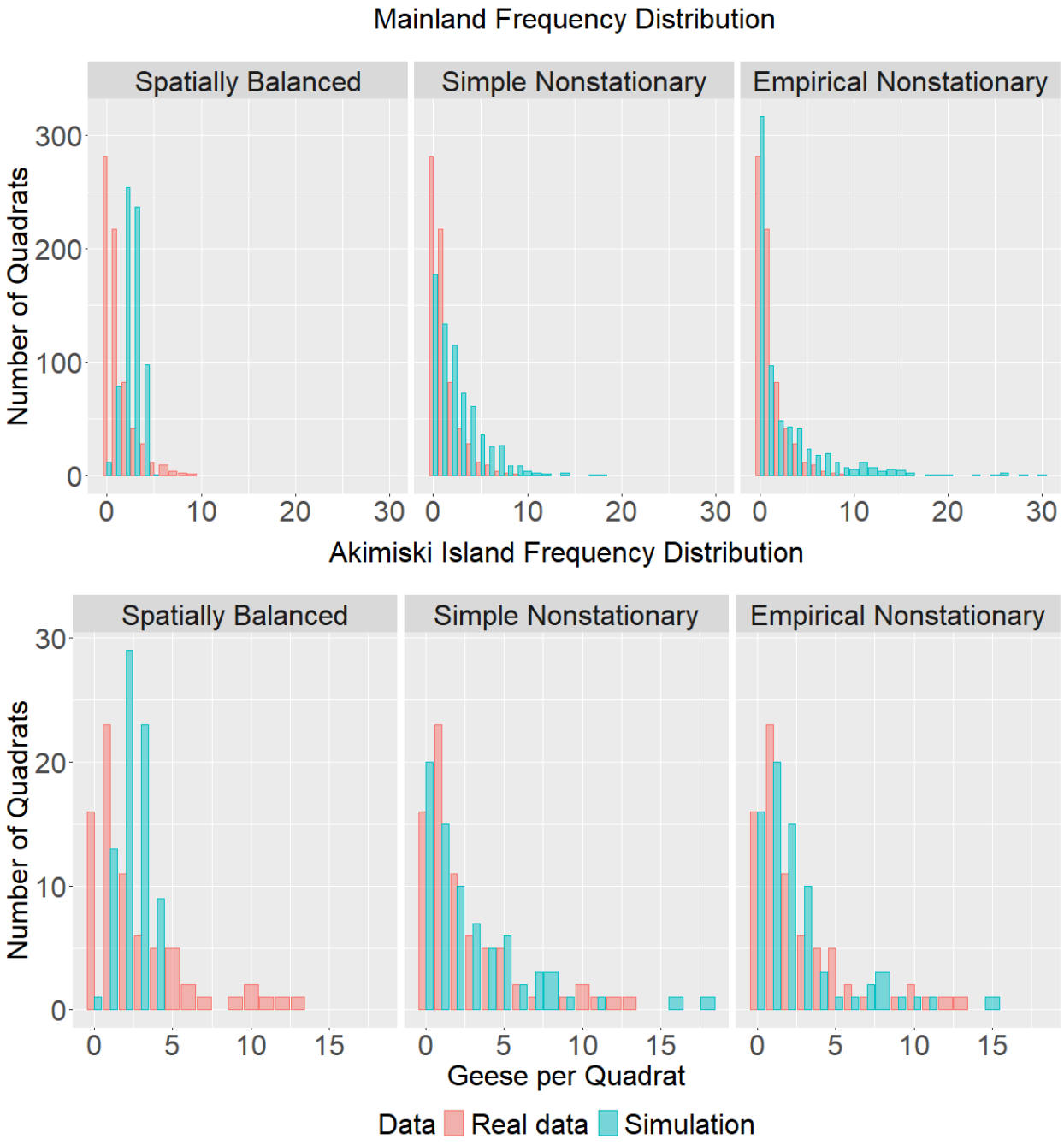

Figure 7. The frequency distribution of the number of geese per quadrat for the real data and the three simulation scenarios.

4.0 Discussion

4.1 Evaluation of abundance estimation models

In addition to good survey design, reliable inferences about populations require careful consideration of the analytical methods. Indeed, deciding among analysis methods is an issue that cannot be understated. Model-based and design-based methods both have their benefits and uses, though selecting one needs careful consideration (Dumelle et al., 2022). Out of the four abundance estimation models evaluated, I found that the untransformed empirical bayesian kriging (EBK; model-based) had the highest accuracy in estimating Canada goose population abundance, followed (in order) by areal interpolation (model-based) and the ratio estimator (design-based), and transformed empirical Bayesian kriging (EBKT; model-based; Figure 4).

EBK is a geostatistical method with a robust suite of settings allowing for the detection of spatial patterns at small scales (Krivoruchko 2012). As part of my analysis, to allow for this fine-scale detection, the transects for the Canada goose survey were partitioned into sub-block quadrats as a centroid-based sample design. Areal interpolation used the same sample units as EBK; however it was not as accurate at estimating population size across all three simulations (Figure 4). Grid-based areal interpolation tends to have improved accuracy over centroid-based areal interpolation, likely due to its more robust semivariogram (Liu & Yu, 2008; Liu et al., 2008). Thus, the lower accuracy of areal interpolation in comparison to untransformed EBK may be due, at least in part, to my centroid-based transect-quadrat sample design.

At the other end of the spectrum, EBKT consistently produced the least accurate estimates across simulations. I surmise this accuracy difference between EBKT and EBK is a result of the differences in which semivariograms are generated between these two approaches (Krivoruchko

2012). Untransformed EBK is modelled using an intrinsic random function; however, when a transformation is applied to EBK (EBKT), a simple kriging model is used (Krivoruchko 2012). As such, EBKT does not generate multiple semivariograms in the same way as EBK, likely leading to lower accuracy to estimate population abundance, especially where organism abundance is nonstationary (Figure 4).

Whereas kriging methods take advantage of the spatial autocorrelation in abundance, ratio estimators can be constrained by such autocorrelation. Indeed, for ratio estimators, independence of sampling units is a fundamental assumption. In my analysis, the ratio estimator overestimated abundance for the nonstationary simulations (Figure 4). Since the ratio estimator was calculated using entire transects as sample units rather than transects partitioned into quadrats (to help meet the assumption of independence), the ratio estimator was computed at a coarser spatial scale than the other methods. This coarser resolution may explain why the ratio estimator consistently overestimated abundance, as larger sample units are less likely to detect fine scale spatial patterns.

In estimating organism abundance, precision is also important, as it can govern the power for detecting change. Indeed, type II errors loom large in conservation (Caughley and Gunn 1996). With regard to the precision of these population estimates, precision generally decreased with increased nonstationarity, which is a common issue in population estimation (Rollinson et al., 2021; Murphy & Jarzyna, 2023; Figure 7). Not surprisingly, methods using the spatially balanced simulation generated the most precise estimated population size across estimators, followed by the simple nonstationary simulation and lastly the empirical nonstationary simulation (Figure 4). This decrease in precision is to be expected as data points become more irregularly dispersed.

This was counter to my prediction that the estimates using the empirical nonstationary simulation would be more precise than the simple nonstationary simulation due to the empirical nonstationary simulation's realistic point distribution. The empirical nonstationary simulation exhibited the highest point aggregation and spatial autocorrelation across simulations (Figure 5; Figure 6). This may have compounded the reduction of precision, as clustered distributions can cause less precise population estimates (Takashina et al., 2018). In addition, while the simple nonstationary cluster locations were randomly generated, the cluster radiuses and distances between clusters were predetermined, which could create an artificial sense of uniformity and may have inflated this increase in precision in comparison to the empirical nonstationary simulations.

The areal interpolation simulation performed with lower precision than EBK, which was similar for the real data analysis (Figure 4; Figure 2). Indeed, the areal interpolation simulations for the mainland exhibited substantially higher standard deviations than EBK and EBKT (Figure 4). Given that our dataset had a Poisson distribution, and that the overdispersed areal interpolation model allows for such data, I expected that areal interpolation would have performed more precisely than the EBK estimators. On the other hand, EBK assumes data have a Gaussian distribution, but it performed well despite the zero-inflated Poisson distribution.

This imprecision for areal interpolation appeared sensitive to population size. Areal interpolation was highly imprecise when using the spatially balanced point distribution for the mainland study area, as evident by the large error bars (Figure 4). However, this outcome did not occur for the same artificial distribution at the lower population size of 50,000 simulated geese (Appendix 6). This difference in precision may have been due to the high simulated population

size of 100,000 birds having a higher consistency of distances between points. Furthermore, the areal interpolation model parameterization did not always include a "Partial Sill" parameter when using the spatially balanced data. To run this method, I had to specify a low "Partial Sill" dummy variable to run the method, which may have decreased the precision.

4.2 Analytical methods & assumptions

Independent of the simulations, each method had its advantages and disadvantages (Table 1). For the design-based ratio estimator, population estimates and confidence intervals were straightforward to compute and they were consistent with the survey sample design, but the inference was not spatial. In contrast, EBK had the advantages of enhanced accuracy and spatially explicitness, but estimating the population and precision was not straightforward. Indeed, design-based methods are often much more computationally efficient than model-based methods (Dumelle et al., 2022). The ratio estimator (Stehman & Salzer, 2000) has been applied to many studies, although much less so in large-scale avian surveys. The ratio estimator has been used, for example, to estimate the abundance of murrelets (Kirchhoff 2008; Kirchhoff et al., 2014), salamanders (Pehek & Stanley, 2015), pelagic finfish (Taylor 2015), rare vegetation species (Krening et al., 2021; Althaus 2022) trees and forest volume (Ringvall et al., 2007; Persson et al., 2022).

In my analysis, the ratio estimator was useful and simple because it was a model based solely on sample design, that is, the ratio estimator is based on sample scale of entire transects. This can be useful because the resulting estimates are true to the sample design. However, this may limit the model's ability to detect finer-scale patterns in abundance and distribution that may be of interest to wildlife managers. The ratio estimator is also relatively assumption-free; the method

does not require observations to be normally distributed, to have equal variance or randomly distributed observations (Table 1; Stehman and Salzer 2000). This assumption-free aspect is inherent to design-based methods, as the sampling protocol is the only source of stochasticity (Brus & Guijter, 1997). However, the low-assumption element for design-based methods may serve as a hinderance, particularly in contrast to methods that capitalize on nonstationarity as a source of information (Ver Hoef 2008). The lack of spatial inference and nonstationarity assumption may be the reason why in my evaluation, the ratio estimator consistently underestimated the true population size (Figure 3).

Although population estimates from the ratio estimator were consistently underestimated, the assumption-free nature of the ratio estimator and strong design-based validity of the method are appealing. The ratio estimator also followed a similar trend as the untransformed EBK estimator for the the real survey data (Figure 1). Consequently, the ratio estimator had value for comparing population trends among methods.

In contrast, classical kriging carries a key assumption. These geospatial techniques assume spatial homogeneity, meaning the semivariogram and mean are equal at all locations (Krivoruchko 2012). Indeed, such classical geostatistical models assume that the data are Gaussian distributed and originate from a stationary process; however, EBK can handle moderate nonstationarity (Gribov & Krivoruchko, 2020). Model-based estimators often require several assumptions to be met; violating these assumptions can introduce error. Careful consideration is needed to ensure the resulting model validity (Brus & Guijter, 1997). A key assumption for EBK is the data-dependent prior distribution (Krivoruchko & Gribov, 2019). This means that EBK assumes spatial relationships are based on initial data characteristics. Inherently, the Canada

goose observation data do not meet the assumption of spatial homogeneity, as different patches of land have varying densities related to multiple external factors, such as habitat, social structure, and weather (Craven & Rusch, 1983; Caithamer et al., 1992). Consequently, this assumption is often violated in real populations (Gribov & Krivoruchko 2020).

4.3 Akimiski Island discrepancies

The simulations showed that, compared to the mainland, population estimates of Canada geese on Akimiski Island differed from the mainland with respect to accuracy and precision (Figure 4; Figure 5; Figure 6). These differences are likely attributable to Akimiski Island's transect design and smaller study area.

The transects on the island, first established in 1990, appear to reflect a subjectively placed sample layout that captured generally observed patterns in nesting goose distribution (ECCC 2017). Historical survey data indicate that Canada goose density on the island is often highest in the northwestern shores and the majority of the transects on Akimiski Island are positioned on the north end of the island. Subjectively positioned samples may not be as effective as systematic sampling or random sampling for tracking changes in abundance and distribution. Samples positioned based on historical density on the island may also not be as effective if nesting geese distribution changes over time, for reasons such as herbivory, habitat quality, and climate (Si et al., 2011; Jenson et al., 2008; Morrissette et al., 2010).

On the other hand, inadequate coverage of densely populated areas could also be a source of inaccuracy for Akimiski Island. The transects on the island cover 2.5% of the study area, which is higher than the mainland at 1.7%. However, only 2 of the 7 Akimiski Island transects overlap with the northwestern historically high-density area. This accounts to 2 out of 7 transect samples

for design-based methods (ratio estimator) and 10 out of 75 sub-transect quadrats for model-based methods (EBK and areal interpolation). In comparison, the mainland study area has a total of 58 transects and 756 quadrats. I surmise that the low sample coverage of high-density areas on Akimiski Island is a source of imprecision; increasing sampling in high density strata is common in survey designs, especially in stratified random sampling, as a means to improve overall precision of estimates (Cochran 1977; Baillargeon & Rivest, 2009). If Akimiski Island's transects were repositioned to an improved systematic design, the precision of population estimates of Canada geese would likely improve.

The total area of Akimiski Island may have also impacted the accuracy and precision of abundance estimates. While simulated population densities between island and mainland were similar, the smaller study area on Akimiski Island left less space for simulated spatial patterns. This was especially the case for the simple nonstationary simulation, as the smaller study area constrained potential locations for randomly positioned clusters of points. Consequently, this highly clustered population in tandem with an unrepresentative sample likely diminished the accuracy and precision of these estimates (Figure 4). If the survey design on Akimiski Island was modified to resemble that on the mainland, based on systematically spaced transects, post-survey analysis would likely better detect spatial patterns and abundance and changes through time.

4.4 Aerial survey design & detectability

In aerial surveys of wildlife abundance, inaccuracy may stem from sample design, observer skill, and visibility conditions. A sound aerial survey design is crucial because factors such as counting bias and sightability strongly influence the results (Krebs 1989). Apart from the model induced inaccuracies discussed above, the sampling itself can be a major source of inaccuracy. In

my thesis, the simulations allowed for perfect detection, but real surveys rely on certain conditions.

For line transects to generate accurate results, four assumptions need to be met. First, no animals should be missed in each quadrat searched. Second, the presence of animals should be independent of the observer (e.g. animals found along transects do not flush unnoticed). Third, there should be no measurement or rounding errors. Lastly, each observation should be independent of each other (Anderson 1979). Regarding the assumption that no animals are missed, an experienced survey crew is likely to reduce such errors, though there may be unavoidable missed counts due to poor weather conditions and land cover. To account for detection rates, double observer methods can be used to estimate imperfect detection and correct estimates accordingly to improve accuracy (e.g. Roy et al., 2022). Pertaining to observations being independent of each other and the observer, the aircraft flown for the Canada goose surveys are likely to make geese flush from their initial location before being sighted. Indeed, apart from visibility conditions, sighting probability likely depends on the response of the animal to the observer (Anderson 1979). Reducing aircraft noise is not practical for these high-cost, remote area surveys. However, this error is reduced for the Canada goose surveys by timing aircraft surveys during the nesting season, as nesting birds are more invested in their nests and less prone to flushing (Lewis et al., 2019). Analytical methods that incorporate imperfect detection and geostatistics may further improve accuracy of real data estimates. Consequently, at least for Canada geese, timing surveys around nesting times is likely the most practical way to reduce this form of error. The animal response to aircraft is an issue that likely applies to all aerial transect surveys on mobile species.

Estimator	Summary	Pros	Cons	Reference
Ratio estimator	• Sample design-based • Density- ratio accounting for uneven transect lengths	• Can be automated • Accounts for uneven sample area	• Does not account for spatial autocorrelation • Large sample scale (transect)	Stehman & Salzer (2000)
Areal interpolation	• Geospatial prediction • Kriging model using data aggregated over polygons	• Allows discrete counts • Allows Poisson count data • Manual modelling	• No automation option for modelling	Krivoruchko et al. (2011) ESRI (2023)
Empirical Bayesian kriging (EBK)	• Geospatial prediction • Kriging model with robust modelling options • Accounts for errors in classical kriging models	• Designed for large datasets • Modelling can be automated • Transforms data to Gaussian distribution • Robust modelling parameters • Accounts for errors in classical kriging through modelling multiple semivariograms	• Not meant for quadrat count data • Uses Gaussian distributed data, whereas Canada geese display a Poisson distribution	Gribov & Krivoruchko (2020) Krivoruchko & Gribov (2019) Krivoruchko (2012)

Table 1. The anticipated pros and cons of each of three population estimator methods[1].

[1] Transformed EBK (EBKT) is not included as it is the same method as EBK with a transformation applied.

5.0 Management implications, future considerations, and conclusions

A fundamental premise of sampling is that the samples are representative of the larger population. For the Canada goose Mississippi Flyway surveys, the survey design would likely be improved if the systematic transect layout (used on the mainland since 2016) were applied to Akimiski Island (Figure 1). This would increase comparability between the two study areas, and likely improve the accuracy and precision of estimates of the abundance of Canada geese on the island.

The EBKT population estimator was computed using the same selection of model parameters for each simulation run. Due to the size of the dataset and the many available parameters for EBK, I could not test out all parameter combinations for EBKT; it would be beneficial for additional studies to examine in more detail why the transformed and untransformed appear to behave differently. Further testing on EBK using a range of options for transformations when comparing simulated population estimates would be useful. Out of all the estimators tested, the untransformed EBK estimator was the most accurate and precise at predicting true population size (Figure 4). This indicated that nonstationarity was a likely strong factor for the detection of true population size. The ratio estimator generally followed the same trends as EBK, albeit with less accuracy (Figure 4). Thus, for this population of Canada geese, it may be useful to employ EBK in future analysis, while comparing trends with the design-based estimator.

When performing population estimates, it is crucial to carefully consider precision and accuracy. However, for some purposes, where the detection of trends is the indicator of interest, population monitoring may accept some level of inaccuracy as long as the bias remains similar across surveys. In these scenarios, precision may be the key determinant for detecting change.

Conversely, accurate estimates of absolute abundance are likely critical for harvest allocation decisions as well as for tracking minimum population size for conservation targets. Even so, precision cannot be overlooked as the inability to discern trends can be serious, especially for species in decline. Gaining reliable knowledge from wildlife surveys means that scientists and managers need to consider not only the outcome but the uncertainties and limitations of these analytical methods.

Bibliography

Abramowitz, M., & Stegun, I. A. (1968). Handbook of mathematical functions with formulas, graphs, and mathematical tables (Vol. 55). US Government printing office. pp 374

Alisauskas, R. T., Drake, K. L., & Nichols, J. D. (2009). Filling a void: abundance estimation of North American populations of arctic geese using hunter recoveries. *Modeling demographic processes in marked populations*, 463-489. https://doi.org/10.1007/978-0-387-78151-8_20

Althaus, K. N. (2022). Understanding rare species in California: an assessment of camatta canyon amole (*Hooveria purpurea var. reducta*) and a meta-analysis of California rare plants in literature (Doctoral dissertation, California Polytechnic State University). https://doi.org/10.15368/theses.2022.122

Anderson, D. R., Laake, J. L., Crain, B. R., & Burnham, K. P. (1979). Guidelines for line transect sampling of biological populations. *The Journal of Wildlife Management*, *43*(1), 70-78. https://doi.org/10.2307/3800636

Aubry, P., & Francesiaz, C. (2022). On comparing design-based estimation versus model-based prediction to assess the abundance of biological populations. *Ecological Indicators*, 144, 109394. http://dx.doi.org/10.1016/j.ecolind.2022.109394

Baillargeon, S., & Rivest, L. (2009). A general algorithm for univariate stratification. *Int Statistical Rev*, *77*(3), 331-344. https://doi.org/10.1111/j.1751-5823.2009.00093.x

Bazely, D. R., & Jefferies, R. L. (1986). Changes in the composition and standing crop of salt-marsh communities in response to the removal of a grazer. *The Journal of Ecology*, 693-706. https://doi.org/10.2307/2260392

Brook, R. W., Leafloor, J. O., Abraham, K. F., & Douglas, D. C. (2015). Density dependence and phenological mismatch: consequences for growth and survival of sub-arctic nesting Canada Geese. *Avian Conservation & Ecology*, *10*(1). https://doi.org/10.5751/ACE-00708-100101

Brook, R., Brown, G., & Badzinski, S. (2018). Preliminary spring survey results for interior Canada geese. Unpublished manuscript, *Environment and Climate Change Canada:* 1-8.

Brus, D. J., & De Gruijter, J. J. (1997). Random sampling or geostatistical modelling? Choosing between design-based and model-based sampling strategies for soil (with discussion). Geoderma, 80(1-2), 1-44. https://doi.org/10.1016/S0016-7061(97)00072-4

Buij, R., Melman, T. C., Loonen, M. J., & Fox, A. D. (2017). Balancing ecosystem function, services and disservices resulting from expanding goose populations. Ambio, 46, 301-318. https://doi.org/10.1007/s13280-017-0902-1

Caraco, T. (1980). Stochastic dynamics of avian foraging flocks. The American Naturalist, 115(2), 262-275.

Caughley, G., & A. Gunn. (1996). Conservation Biology in Theory and Practice. Blackwell Science, Cambridge, Massachusetts, U.S.A.

Caithamer, David F., Pritchert, R. D., Gates, R. J., & Tacha, T. C. (1992). Habitat use by the Mississippi Valley population of Canada geese. *Transactions-of-the-Illinois-State-Academy-of-Science*, *85*, 1–2.

Clark, I. (1978). *Geostatistics. The Royal School of Mines Journal*. https://www.kriging.com/RSMA1978/.

Cochran, W. G. (1977). Sampling techniques (3rd ed., pp. 101–103). John Wiley & Sons, Inc.

Craven, S. R., & Rusch, D. H. (1983). Winter distribution and affinities of Canada geese marked on Hudson and James Bays. *The Journal of Wildlife Management*, *47*(2), 307-319. https://doi.org/10.2307/3808503

Cressie, N. (1993). Spatial prediction and kriging. *Statistics for Spatial Data,* (pp. 119-120). https://doi.org/10.1002/9781119115151.ch3

Dorazio, R. M. (2007). On the choice of statistical models for estimating occurrence and extinction from animal surveys. *Ecology*, *88*(11), 2773-2782. https://doi.org/10.1890/07-0006.1

Dragulescu, A., & Arendt, C. (2020). xlsx: read, write, format Excel 2007 and Excel 97/2000/XP/2003 Files. *R Package Version*, *0*(6), 5. https://rdrr.io/cran/xlsx/

Dumelle, M., Higham, M., Ver Hoef, J. M., Olsen, A. R., & Madsen, L. (2022). A comparison of design-based and model-based approaches for finite population spatial sampling and inference. *Methods in Ecology and Evolution*, *13*(9), 2018-2029. https://doi.org/10.1111/2041-210X.13919

ECCC. (2017). Waterfowl survey list | Canada goose breeding pair surveys. Environment and Climate Change Canada. https://www.canada.ca/en/environment-climate-change/services/bird-surveys/waterfowl/list.html

ESRI. (2024a). ArcPy. ArcGIS Python libraries. https://www.esri.com/en-us/arcgis/products/arcgis-python-libraries/libraries/arcpy

ESRI. (2024b). Empirical bayesian kriging (geostatistical analyst). ArcGIS Pro documentation. https://pro.arcgis.com/en/pro-app/latest/tool-reference/geostatistical-analyst/empirical-bayesian-kriging.htm

ESRI. (2024c). What is Empirical Bayesian Kriging? ArcGIS Pro documentation. https://pro.arcgis.com/en/pro-app/latest/help/analysis/geostatistical-analyst/what-is-empirical-bayesian-kriging-.htm

ESRI. (2024d). What is areal interpolation? ArcGIS Pro documentation. https://pro.arcgis.com/en/pro-app/latest/help/analysis/geostatistical-analyst/what-is-areal-interpolation.htm

Green, N. S., Wildhaber, M. L., & Albers, J. L. (2022). Interaction between transect design and animal distribution in distance sampling of deer. *Wildlife Society Bulletin*, *46*(5), e1368. https://doi.org/10.1002/wsb.1368

Gribov, A., & Krivoruchko, K. (2020). Empirical Bayesian kriging implementation and usage. *Science of The Total Environment*, *722*, 137290. https://doi.org/10.1016/j.scitotenv.2020.137290

Harris, C. R., Millman, K. J., Van Der Walt, S. J., Gommers, R., Virtanen, P., Cournapeau, D., ... & Oliphant, T. E. (2020). Array programming with NumPy. *Nature*, *585*(7825), 357-362. https://doi.org/10.1038/s41586-020-2649-2

Hijmans, R. J. (2023). Geographic data analysis and modeling. [R package raster version 3.6-20]. https://cran.r-project.org/web/packages/raster/index.html

Jenson, R. A., Madsen, J., O'Connell, M., Wisz, M. S., Tømmervik, H., & Mehlum, F. (2008). Prediction of the distribution of Arctic-nesting pink-footed geese under a warmer climate scenario. *Global Change Biology*, *14*(1), 1-10. https://doi.org/10.1111/j.1365-2486.2007.01461.x

Johnston, K., Ver Hoef, J. M., Krivoruchko, K., & Lucas, N. (2004). Using ArcGIS geostatistical analyst. (Vol. 380). Redlands: Esri. pp 257

Kéry, M. (2002). Inferring the absence of a species: a case study of snakes. *The Journal of Wildlife Management*, *66*(2), 330-338. https://doi.org/10.2307/3803165

Kirchhoff, M. D. (2008). Methodological considerations for at-sea monitoring of Brachyramphus murrelets in Glacier Bay, Alaska. *Final Report, Feb*.

Kirchhoff, M. D., Lindell, J. R., & Hodges, J. I. (2014). From critically endangered to least concern?—A revised population trend for the Kittlitz's Murrelet in Glacier Bay, Alaska. *The Condor*, *116*(1), 24-34. https://doi.org/10.1650/CONDOR-13-123.1

Krebs, C. (1989). Ecological methodology. Harper & Row.

Krening, P. P., Dawson, C. A., Holsinger, K. W., & Willoughby, J. W. (2021). A sampling-based approach to estimating the minimum population size of the federally threatened Colorado hookless cactus (*Sclerocactus glaucus*. *Natural Areas Journal*, *41*(1), 4-10. https://doi.org/10.3375/043.041.0102

Krivoruchko, K., Gribov, A., & Krause, E. (2011). Multivariate areal interpolation for continuous and count data. Procedia Environmental Sciences, 3, 14-19. https://doi.org/10.1016/j.proenv.2011.02.004

Krivoruchko, K. (2012). Empirical Bayesian kriging implemented in ArcGIS Geostatistical Analyst. *Esri*. https://www.esri.com/news/arcuser/1012/empirical-byesian-kriging.html

Krivoruchko, K., & Gribov, A. (2019). Evaluation of empirical Bayesian kriging. *Spatial Statistics*, *32*, 100368. https://doi.org/10.1016/j.spasta.2019.100368

Kuijper, D. P. J., Ubels, R., & Loonen, M. J. J. E. (2009). Density-dependent switches in diet: a likely mechanism for negative feedbacks on goose population increase?. *Polar Biology*, 32, 1789-1803.

Lancia, R. A., Kendall, W. L., Pollock, K. H., & Nichols, J. D. (2005). Estimating the number of animals in wildlife populations. 106-153.

Leafloor, J. O., Hill, M. R., Rusch, D. H., Abraham, K. F., & Ross, R. K. (2000). Nesting ecology and gosling survival of Canada Geese on Akimiski island, Nunavut, Canada. *Towards conservation of the diversity of Canada Geese* (ed K.M. Dickson), Canadian Wildlife Service Occasional Papers No. 103. Ottawa.

Lewis, T., Swaim, M., Schmutz, J., & Fischer, J. (2019). Improving population estimates of threatened spectacled eiders: correcting aerial counts for visibility bias. *Endangered Species Research*, *39*, 191-206. https://doi.org/10.3354/esr00959

Link, W. A., & Sauer, J. R. (1997). Estimation of population trajectories from count data. *Biometrics*, 488-497.

Link, W. A., & Sauer, J. R. (2002). A hierarchical analysis of population change with application to Cerulean Warblers. Ecology, 83(10), 2832-2840.

Liu X., & Liu Y. (2008). The accuracy assessment in areal interpolation: An empirical investigation. *Science in China Series E: Technological Sciences*, *51*:62-71.

Liu X., Kyriakidis P., Goodchild M. (2008). Population estimation using regression and area-to-point residual kriging. *International Journal of Geographical Information Science*, *22*(4): 431-447. https://doi.org/10.1080/13658810701492225

Luukkonen, D., Leafloor, J., Abraham, K., Badzinski, S., Baldwin, F., Brook, R., Kelley, J., Naylor, L., Phelps, A., Raedeke, A., & Horn, K. (2017). A Management plan for Mississippi Flyway Canada Geese. *Reports prepared by the Mississippi Flyway Council Technical Section Canada Goose Committee, Mississippi Flyway Council, USA*.

McAlister, M. A., Moorman, C. E., Meentemeyer, R. K., Fuller, J. C., Howell, D. L., & DePerno, C. S. (2017). Using landscape characteristics to predict distribution of temperate-breeding Canada geese. *Southeastern Naturalist*, *16*(2), 127–139. https://doi.org/10.1656/058.016.0201

McDonald, L. L. (2004). Sampling rare populations. *Sampling rare or elusive species: concepts, designs, and techniques for estimating population parameters*, 11-42.

McCallum, H. (2008). *Population parameters: estimation for ecological models* (pp. 48, 313). John Wiley & Sons. https://doi.org/10.1002/9780470757468

McKinney, W. (2010). Data structures for statistical computing in Python. In *SciPy* (Vol. 445, No. 1, pp. 51-56). https://doi.org/10.25080/Majora-92bf1922-00a

Mech, L. (1966). The wolves of Isle Royale (pp. 37–39). United States, Department of the Interior.

Morrissette, M., Bêty, J., Gauthier, G., Reed, A., & Lefebvre, J. (2010). Climate, trophic interactions, density dependence and carry-over effects on the population productivity of a migratory Arctic herbivorous bird. *Oikos*, *119*(7), 1181–1191. https://doi.org/10.1111/j.1600-0706.2009.18079.x

Murphy, S., & Jarzyna, M. (2023). Spatial and temporal non-stationarity in long-term population dynamics of over-wintering birds of North America. *Ecology and Evolution*, *13*(3), e9781. https://doi.org/10.22541/au.165890198.84826153/v1

Pearse, A. T., Dinsmore, S. J., Kaminski, R. M., & Reinecke, K. J. (2008). Evaluation of an aerial survey to estimate abundance of wintering ducks in Mississippi. *The Journal of Wildlife Management*, *72*(6), 1413-1419.

Pebesma E., Bivand R (2023). Spatial data science with applications in R. Chapman & Hall. https://r-spatial.org/book/

Pehek, E., & Stanley, S. C. (2015). A case study of urban streamside salamander persistence in Staten Island, NY. *Cities and the Environment (CATE)*, *8*(1), 4.

Persson, H. J., Olofsson, K., & Holmgren, J. (2022). Two-phase forest inventory using very-high-resolution laser scanning. *Remote Sensing of Environment*, *271*, 112909. https://doi.org/10.1016/j.rse.2022.112909

Peterson, J. T., & Bayley, P. B. (2004). A Bayesian approach to estimating presence when a species is undetected. In T. William (Ed.), *Sampling rare or elusive species*. Island Press Washington, DC. pp. 177-188. https://archive.org/details/samplingrareorel0000unse/page/172/mode/2up

Peterson, R., Thomas, N., Thurber, J., Vucetich, J., & Waite, T. (1998). Population limitation and the Wolves of Isle Royale. *Journal of Mammalogy*, *79*(3), 828-841. https://doi.org/10.2307/1383091

R Core Team. (2023). R: a language and environment for statistical computing. R foundation for statistical computing, Vienna, Austria. https://www.R-project.org.

Reed, D. H. (2008). The effects of population size on population viability: from mutation to environmental catastrophes. *Conservation Biology: Evolution in Action*, 16-34. https://doi.org/10.1093/oso/9780195306798.003.0002

Reiter, M. E., Anderson, D. E., Raedeke, A. H., Humburg D. D. (2013). Species associations and habitat influence the range-wide distribution of breeding Canada geese (*Branta canadensis interior*) on western Hudson Bay. *Waterbirds*, *36*(1), 20-33. https://doi.org/10.1675/063.036.0105

Ringvall, A., Snäll, T., Ekström, M., & Ståhl, G. (2007). Unrestricted guided transect sampling for surveying sparse species. *Canadian Journal of Forest Research, 37*(12), 2575-2586. https://doi.org/10.1139/X07-074

Rollinson, C. R., Finley, A. O., Alexander, M. R., Banerjee, S., Dixon Hamil, K.-A., Koenig, L. E., Locke, D. H., DeMarche, M. L., Tingley, M. W., Wheeler., C. Youngflesh., & E. F. Zipkin, K. (2021). Working across space and time: nonstationarity in ecological research and application. *Frontiers in Ecology and the Environment*, *19*(1), 66-72. https://doi.org/10.1002/fee.2298

Roy, C., Gilliland, S. G., & Reed, E. T. (2022). A hierarchical dependent double-observer method for estimating waterfowl breeding pairs abundance from helicopters. *Wildlife Biology*, *2022*(1). https://doi.org/10.1002/wlb3.01003

Royle, J. A., & Nichols, J. D. (2003). Estimating abundance from repeated presence-absence data or point counts. *Ecology*, *84*(3), 777–790. https://doi.org/10.1890/0012-9658(2003)084[0777:eafrpa]2.0.co;2

Royle, J. A., Nichols, J. D., & Kéry, M. (2005). Modelling occurrence and abundance of species when detection is imperfect. Oikos, 110(2), 353-359. https://doi.org/10.1111/j.0030-1299.2005.13534.x

Si, Y., Skidmore, A. K., Wang, T., de Boer, W. F., Toxopeus, A. G., Schlerf, M., Oudshoorn, M., Zwerver, S., van der Jeugd, H., Exo, K.-M., & H. H. Prins (2011). Distribution of barnacle geese *Branta leucopsis* in relation to food resources, distance to roosts, and the location of refuges. *Ardea*, *99*(2), 217-226. https://dx.doi.org/10.5253/078.099.0212

Sólymos, P. (2022). Morisita index of intraspecific aggregation. *vegan: Community Ecology Package*. Version 2.6–4. https://cran.r-project.org/web/packages/vegan/index.html

Stehman, S., & Salzer, D. (2000). Estimating density from surveys employing unequal-area transects. *Wetlands*, *20*(3), 512-519. https://doi.org/10.1672/0277-5212(2000)020<0512:EDFSEU>2.0.CO;2

Takashina, N., Kusumoto, B., Beger, M., Rathnayake, S., & Possingham, H. P. (2018). Spatially explicit approach to estimation of total population abundance in field surveys. *Journal of Theoretical Biology*, *453*, 88-95. https://doi.org/10.1016/j.jtbi.2018.05.013

Tanadini, L. G., & Schmidt, B. R. (2011). Population size influences amphibian detection probability: implications for biodiversity monitoring programs. *Plos One*, *6*(12), e28244. https://doi.org/10.1371/journal.pone.0028244

Taylor, P. R. (2015). Investigating a multi-purpose aerial method for surveying inshore pelagic finfish species in New Zealand. *New Zealand Fisheries Assessment Report*, *36*, 92. http://dx.doi.org/10.13140/RG.2.2.35669.42722

U. S. Fish and Wildlife Service. (2011) Birds of management concern and focal species. https://www.fws.gov/media/birds-management-concern-and-focal-species

Ver Hoef, J. M. (2008). Spatial methods for plot-based sampling of wildlife populations. Environmental and Ecological Statistics, 15, 3-13. https://doi.org/10.1007/s10651-007-0035-y

Virtanen, P., Gommers, R., Oliphant, T. E., Haberland, M., Reddy, T., Cournapeau, D., ... & Van Mulbregt, P. (2020). SciPy 1.0: fundamental algorithms for scientific computing in Python. *Nature methods*, *17*(3), 261-272.

Wickham, H., Averick, M., Bryan, J., Chang, W., McGowan, L. D. A., François, R., & Yutani, H. (2019). Welcome to the Tidyverse. *Journal of Open Source Software*, *4*(43) https://joss.theoj.org/papers/10.21105/joss.01686

Appendix

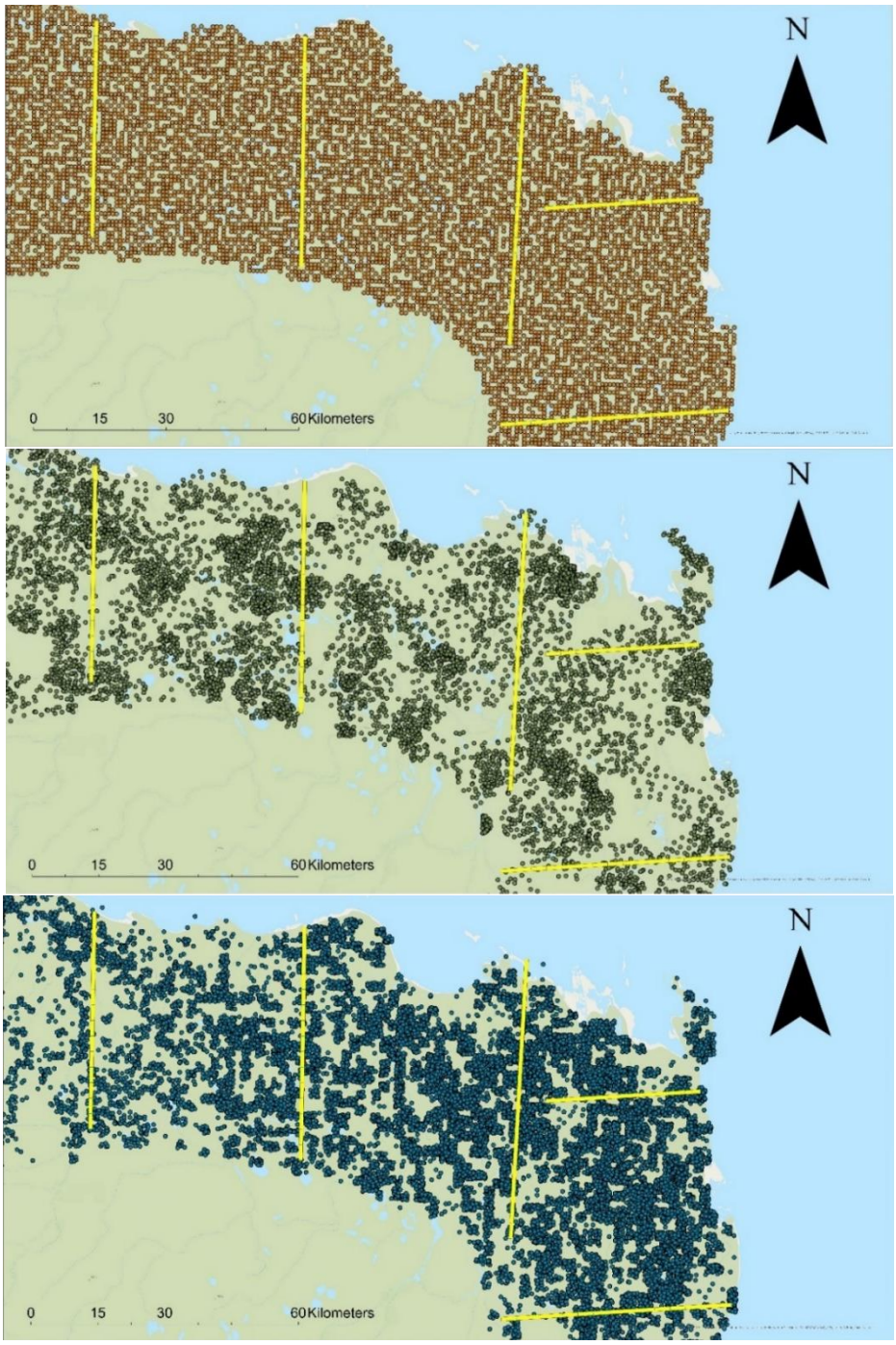

Appendix 1. An example of the simulation for the spatially balanced distribution (top panel), simple nonstationary simulation (middle panel), and empirical nonstationary simulation (bottom panel), on the mainland. The yellow lines represent the survey transects.

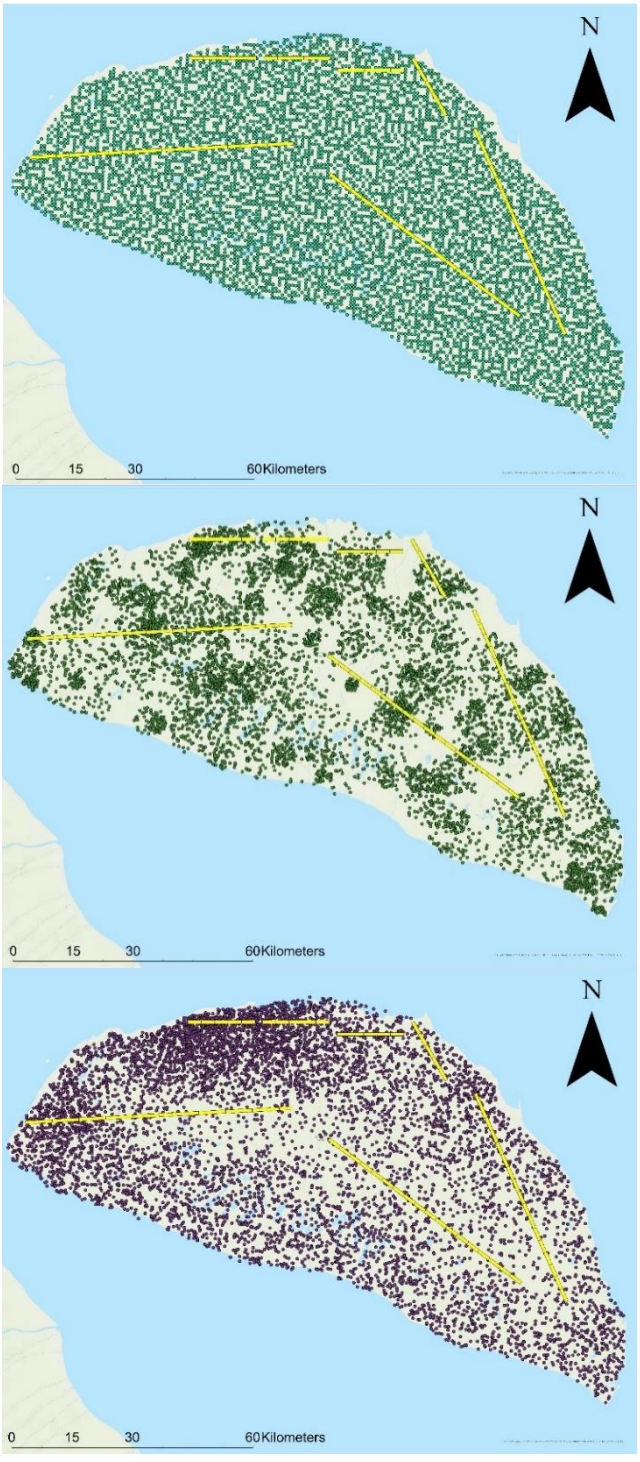

Appendix 2. An example of the simulation for the spatially balanced distribution (top panel), simple nonstationary simulation (middle panel), and empirical nonstationary simulation (bottom panel), on Akimiski Island. The yellow lines represent the survey transects.

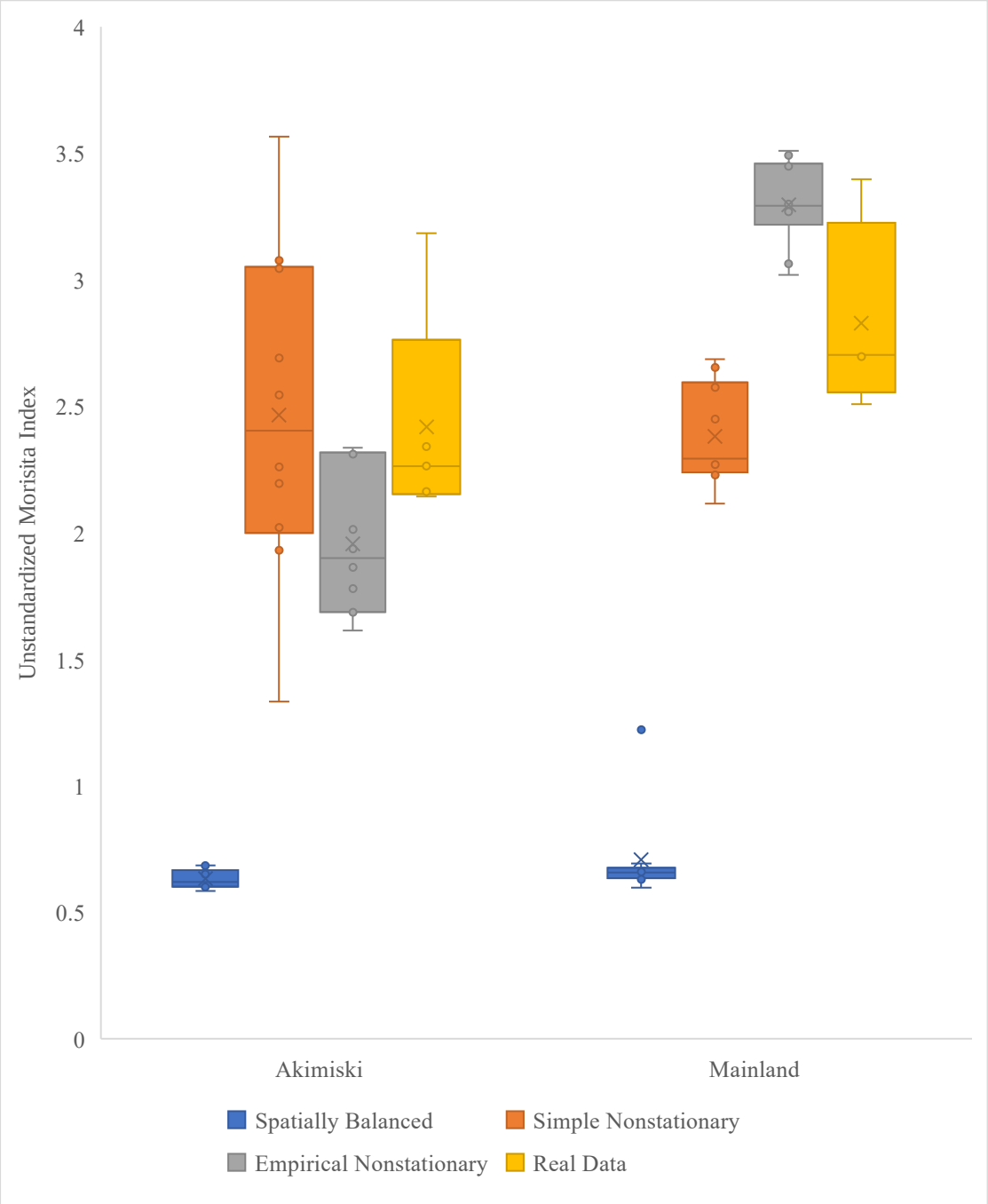

Appendix 3. The unstandardized Morisita index of dispersion for each simulated distribution, for the mainland population of 50,000 and the Akimiski Island population size of 3,750. An I_d between 0-1 indicates uniform distributions while higher values of 0 to *n* indicate clumped distributions (Sólymos 2022).

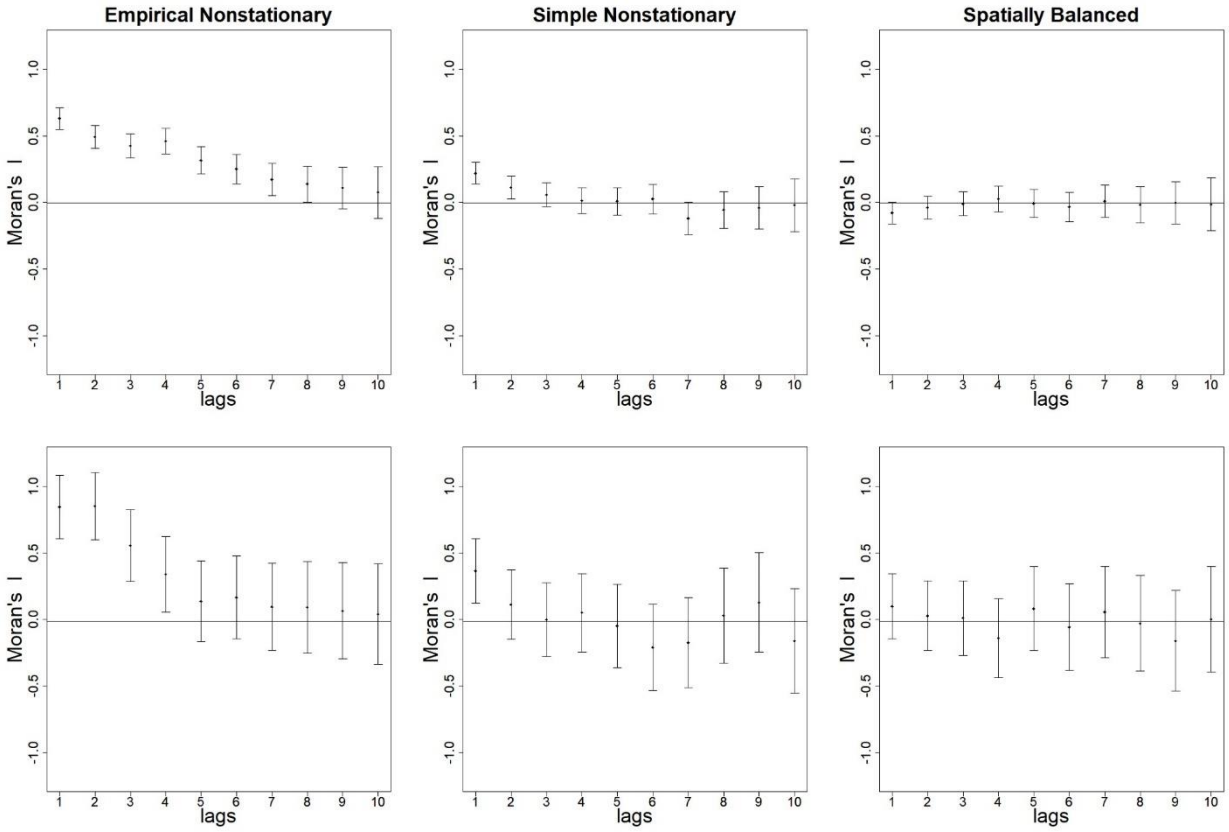

Appendix 4. The Moran's I index for each simulated distribution on the mainland and Akimiski Island, indicating the degree of spatial autocorrelation, for the average observation count per sample units for each simulation (Pebesma & Bivand, 2023). The top panels depict the mainland simulation of 50,000 birds; the bottom panels depict the Akimiski Island simulation of 3,750 birds. Error bars represent the standard deviates of Moran's I.

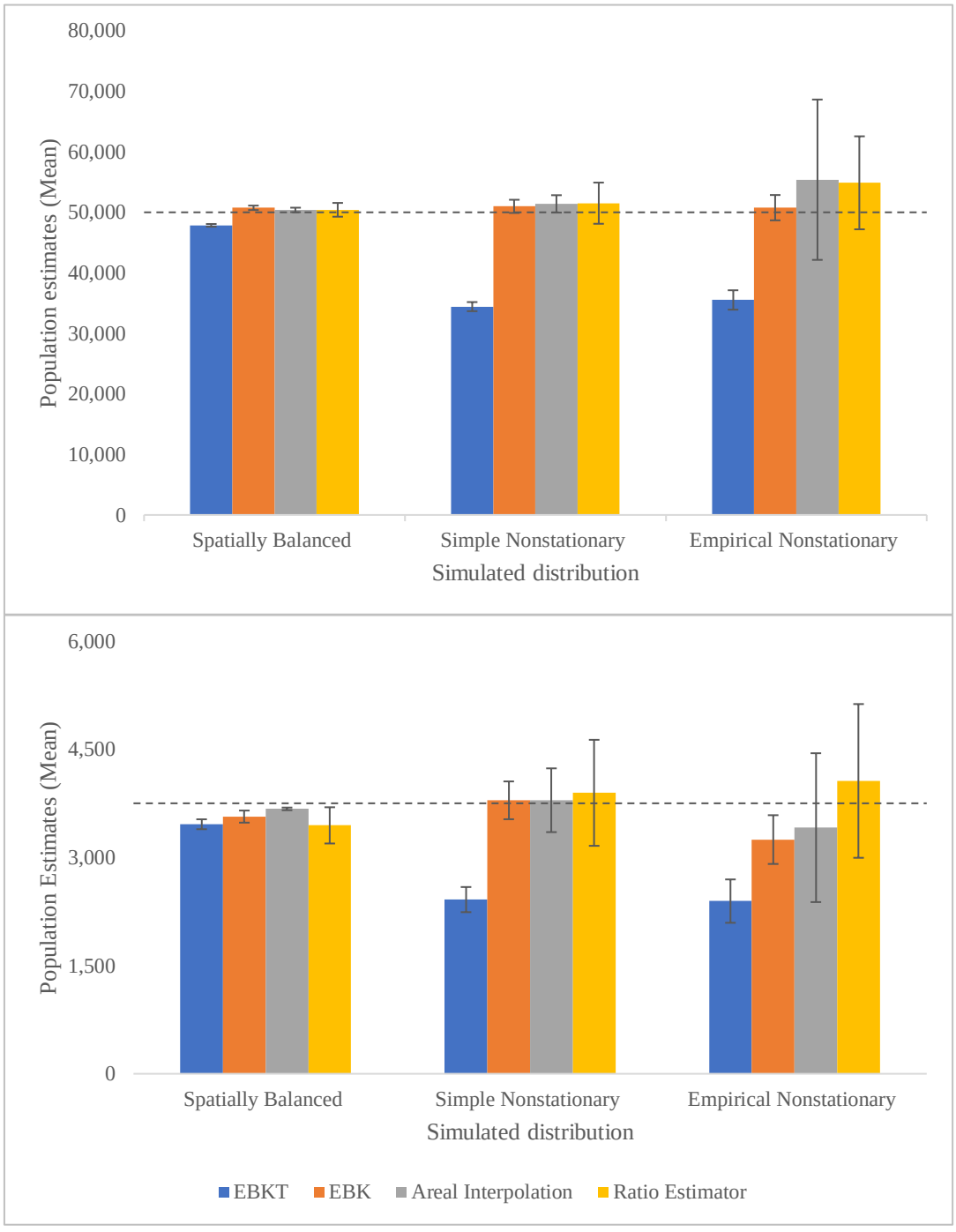

Appendix 5. Mean population estimates averaged from 10 simulations for each of four population estimators and three simulated animal distributions at half the population size (cf. Figure 4). The error bars represent the standard error. The top panel depicts the mainland estimated population sizes using a simulated population of 50,000 points (dashed line), while the bottom panel depicts the Akimiski Island estimated population using a simulated population size of 3,750 points (dashed line).

Appendix 6. The mean biased error for the mainland simulations. The true population size is depicted at Y = 0. The top panel depicts the simulated mainland population of 100,000. The bottom panel depicts the simulated mainland Island population size of 50,000.

Appendix 7. The mean biased error for the Akimiski Island simulations. The true population size is depicted at Y = 0. The top panel depicts the simulated Akimiski Island population of 7,500. The bottom panel depicts the simulated Akimiski Island population size of 3,750.

Subset Size	100
Overlap Factor	4
Number of Simulations	100
Output Surface Type	Prediction
Transformation	None
Semivariogram Type	Power
Neighbourhood Type	Standard Circular
Maximum Neighbors	16
Minimum Neighbors	3
Sector Type	Four Sectors
Radius	8000

Appendix 8. Automated empirical bayesian kriging (EBK) simulation settings; computed using ArcGIS Pro's Geostatistical Analyst, via the ArcPy function EmpiricalBayesianKriging_ga (ESRI 2024a; 2024b).

Subset Size	100
Overlap Factor	3
Number of Simulations	100
Output Surface Type	Prediction
Transformation	Empirical
Semivariogram Type	K-Bessel Detrended
Neighbourhood Type	Standard circular
Maximum Neighbors	16
Minimum Neighbors	3
Sector Type	Four Sectors
Radius	8000

Appendix 9. Automated transformed empirical bayesian kriging (EBKT) simulation settings; computed using ArcGIS Pro's Geostatistical Analyst, via the ArcPy function EmpiricalBayesianKriging_ga (ESRI 2024a; 2024b).